Dynamical Analysis of Regulatory Interactions in the Gap Gene System of *Drosophila melanogaster*

Johannes Jaeger[a], Maxim Blagov[b], David Kosman[c], Konstantin N. Kozlov[b], Manu[a], Ekaterina Myasnikova[b], Svetlana Surkova[b], Carlos E. Vanario-Alonso[a,d], Maria Samsonova[b], David H. Sharp[e] and John Reinitz[a]

[a] Dept of Applied Mathematics and Statistics, and Center for Developmental Genetics, Stony Brook University, Stony Brook, NY 11794-3600, U.S.A.

[b] Department of Computational Biology, Center of Advanced Studies, St. Petersburg State Polytechnical University, St. Petersburg, 194064 Russia

[c] Dept of Biology, University of California, San Diego, CA 92093, U.S.A.

[d]Universidade Federal do Rio de Janeiro, Instituto de Biofísica Carlos Chagas Filho Rio de Janeiro, RJ 21949-900, Brazil

[e] Theoretical Division, Los Alamos National Laboratory, Los Alamos, NM 87545, U.S.A.

Running title:
Dynamical Analysis of Gap Genes

Keywords:
segment determination, segmentation gene network,
gene circuit, non-linear dynamics, simulated annealing

Corresponding Author:
John Reinitz
Dept of Applied Mathematics and Statistics
Stony Brook University
Stony Brook, NY 11794-3600, U.S.A.
Tel: (631) 632 8352
Fax: (631) 632 8490
E-mail: reinitz@odd.bio.sunysb.edu

ABSTRACT

Genetic studies have revealed that segment determination in *Drosophila melanogaster* is based on hierarchical regulatory interactions among maternal coordinate and zygotic segmentation genes. The gap gene system constitutes the most upstream zygotic layer of this regulatory hierarchy, responsible for the initial interpretation of positional information encoded by maternal gradients. We present a detailed analysis of regulatory interactions involved in gap gene regulation based on gap gene circuits, which are mathematical gene network models used to infer regulatory interactions from quantitative gene expression data. Our models reproduce gap gene expression at high accuracy and temporal resolution. Regulatory interactions found in gap gene circuits provide consistent and sufficient mechanisms for gap gene expression, which largely agree with mechanisms previously inferred from qualitative studies of mutant gene expression patterns. Our models predict activation of *Kr* by Cad, and clarify several other regulatory interactions. Our analysis suggests a central role for repressive feedback loops between complementary gap genes. We observe that repressive interactions among overlapping gap genes show anteroposterior asymmetry with posterior dominance. Lastly, our models suggest a correlation between timing of gap domain boundary formation and regulatory contributions from the terminal maternal system.

INTRODUCTION

The segmented body plan of *Drosophila melanogaster* becomes determined during the first three hours of embryogenesis (SIMCOX and SANG, 1983). The genetics of segment determination in the Drosophila blastoderm is very well understood (see AKAM, 1987; INGHAM, 1988, for review). Saturation mutagenesis screens have enabled the isolation of a complete or almost complete set of segmentation genes (NÜSSLEIN-VOLHARD and WIESCHAUS, 1980; NÜSSLEIN-VOLHARD *et al.*, 1987). The zygotic segmentation gene network is a hierarchical dynamical system whose regulatory layers consist of gap, pair-rule and segment-polarity genes (NÜSSLEIN-VOLHARD and WIESCHAUS, 1980). Initial conditions for zygotic segmentation gene expression are given by gradients of the maternal proteins Bicoid (Bcd, Figure 1A,D), Hunchback (Hb, Figure 1B,E) and Caudal (Cad, Figure 1C,F; see ST JOHNSTON and NÜSSLEIN-VOLHARD, 1992, for review). Further maternal input is provided by the terminal maternal system, which regulates segmentation gene expression in the pole regions of the embryo through the zygotic terminal gap genes *tailless (tll)* and *huckebein* (*hkb;* WEIGEL *et al.*, 1990). In the present study, we focus on the regulation of the gap genes *hunchback (hb)*, *Krüppel (Kr)*, *knirps (kni)* and *giant (gt)*, which are expressed in broad domains during the late blastoderm stage (Figure 1G–L).

Detailed genetic and molecular studies have yielded considerable information on the regulatory interactions underlying gap gene expression. Still, our current knowledge of gap gene regulation is incomplete. This is partly due to the ambiguity or absence of experimental data on particular regulatory interactions. However, it is also due to methodological issues concerning the inference of regulatory interactions based on the qualitative study of mutant gene expression in multicellular organisms (*cf.* REINITZ and SHARP, 1995). These issues are rooted in the complexity and the essentially quantitative nature of the dynamical mechanisms of spatial pattern formation. Each blastoderm nucleus has different initial

concentrations of maternal gene products, and hence different initial conditions for zygotic gene expression. This leads to widely and qualitatively different dynamics of zygotic gene expression in different nuclei despite the fact that the underlying regulatory network is the same in each nucleus. A change in the initial conditions in maternal mutants, or in the regulatory circuitry in zygotic mutants, can have unexpected and counterintuitive effects making interpretation of mutant gene expression patterns a highly non-trivial task in all but the most simple cases.

We illustrate the difficulties in interpreting mutant expression patterns with the example of the regulatory effect of Hb on *Kr*. The anterior boundary of the central *Kr* domain is shifted anteriorly in *hb* mutants (JÄCKLE *et al.*, 1986), while *Kr* expression is generally weaker than in wild type embryos (PANKRATZ *et al.*, 1989). Moreover, embryos overexpressing *hb* show posterior expansion of the central *Kr* domain (HÜLSKAMP *et al.*, 1990). Lastly, *Kr* expression is absent in embryos lacking both Bcd and Hb, but is restored in a concentration-dependent manner by reintroducing increasing dosages of Hb (STRUHL *et al.*, 1992; SCHULZ and TAUTZ, 1994). It has been proposed that these effects are due to a dual regulatory role of Hb with activation of *Kr* at low, and repression at high concentrations of Hb (HÜLSKAMP *et al.*, 1990; STRUHL *et al.*, 1992; SCHULZ and TAUTZ, 1994).

However, the above observations can equally well be explained by indirect activation of *Kr* through Kni. The expression domain of *kni*, which encodes a repressor of *Kr* (JÄCKLE *et al.*, 1986; HOCH *et al.*, 1992), expands anteriorly in *hb* mutants (HÜLSKAMP *et al.*, 1990) explaining reduced levels of Kr. The slightly altered posterior *gt* domain in *hb* mutants (ELDON and PIRROTTA, 1991) further complicates interpretation, since Gt is a repressor of both *Kr* (KRAUT and LEVINE, 1991a) and *kni* (ELDON and PIRROTTA, 1991; CAPOVILLA *et al.*, 1992). Expression of *Kr* is restored to high levels in *hb kni* double mutants (HARDING and LEVINE, 1988) further supporting an indirect mechanism. Moreover, embryos overexpressing *hb* lack *kni* expression altogether (KRAUT and LEVINE, 1991a), and posterior extension of

the *Kr* domain in these embryos resembles *Kr* expression in *kni* mutants (JÄCKLE *et al.*, 1986). Lastly, *kni* is widely expressed in embryos lacking Bcd and Hb, but is repressed in a concentration-dependent manner when Hb is reintroduced (STRUHL *et al.*, 1992), which suggests that *Kr* derepression in these embryos is due to increasing repression of *kni*.

The above example reveals three main problems for inferring regulatory mechanisms from qualitative mutant expression data. These are the problems of consistency, uniqueness and completeness.

Consistency of a proposed regulatory mechanism can only be established by keeping track of all regulatory inputs to a specific gene (*cf.* REINITZ and SHARP, 1995). In the case of *Kr*, this involves at least five different regulatory contributions (by Bcd, Cad, Hb, Kni and Gt). Current experimental approaches, however, are limited in their ability to monitor regulatory contributions simultaneously, as such interactions are inferred from mutant expression patterns and it is rarely possible to obtain mutants in more than three genes. Moreover, mutant regulatory systems by definition have an incomplete or otherwise defective set of regulatory interactions. Thus, the regulatory structure of the wild type network must be assembled based on evidence from different experiments. The consistency of such an inferred mechanism can only be established conclusively by testing it in the intact and complete developmental system.

Another problem for interpretation of mutant expression patterns is to establish the uniqueness of a mechanism, *i.e.* to decide whether regulatory interactions are direct or indirect. There are at least two possible regulatory mechanisms which can account for the effect of Hb on *Kr*. Both mechanisms are consistent with available experimental evidence. In such an ambiguous situation, independent evidence can be provided by molecular approaches. Both Hb and Kni have been shown to bind to the *Kr* regulatory region *in vitro* (HOCH *et al.*, 1991, 1992), but the functional importance of such biochemical interactions can only be established *in vivo*. Ideally, this would be achieved by targeted mutation of transcription

factor binding sites in the regulatory region of an endogenous gene. Such an experiment is technically difficult and has not yet been attempted. Alternative approaches involving reporter constructs are subject to two significant complications. First, it is often difficult to establish the regulatory equivalence of such constructs to the endogenous gene. For instance, in *kni* mutants the posterior boundary of the third stripe of *even-skipped (eve)* is intact (Frasch and Levine, 1987), whereas the minimal enhancer for this stripe shows complete derepression between stripes three and seven (Small *et al.*, 1996). Second, regulatory regions used in a construct may contain binding sites for multiple factors (see *Kr* above) or unknown binding sites, which leads to similar ambiguities in interpreting mutant expression patterns as in the case of the endogenous gene.

Lastly, there is a fundamental issue concerning completeness of a proposed regulatory mechanism, which cannot be addressed by experimental approaches alone. The fact that all maternal and gap genes are necessary for correct gap gene expression does not prove that they are also sufficient. It is impossible to prove sufficiency of the inferred mechanism without reconstituting the system *ab initio*, using only well-defined ingredients. Such a reconstitution is obviously impossible by contemporary experimental methods, and hence has to be attempted by using mathematical modeling and computer simulations.

The problems illustrated above show that in order to establish consistency, uniqueness and completeness of a regulatory mechanism, we need a method which allows us to reconstitute wild type gene expression patterns *in silico*, infer underlying regulatory interactions from these wild type patterns, and keep track of all regulatory interactions in all nuclei at all times. The gene circuit method provides such an approach (Mjolsness *et al.*, 1991; Reinitz *et al.*, 1995; Reinitz and Sharp, 1995; Reinitz *et al.*, 1998). It is a data-driven mathematical modeling method whose main aim is to extract information about dynamical regulatory interactions between transcription factors from given gene expression patterns (Figure 2A; Reinitz and Sharp, 1995). This is achieved in four steps: (1) Formulation of a

mathematical modeling framework, (2) collection of gene expression data, (3) fitting of the model to expression data to obtain regulatory parameters, and (4) biological analysis of the resulting gene circuits.

The Drosophila blastoderm permits exceptionally precise modeling, since pattern formation is a consequence of regulatory interactions among segmentation genes only. Segmentation gene mutations affect expression of other segmentation genes, but do not cause any morphological defects before the onset of gastrulation (Merrill *et al.*, 1988). Thus, the internal state of each blastoderm nucleus can be described by concentration levels of transcription factors encoded by segmentation genes. Gap gene circuits include the genes *bcd*, *cad*, *hb*, *Kr*, *gt*, *kni* and *tll*. We do not model RNA explicitly, since it has no known regulatory function in Drosophila segment determination. In addition, there is no tissue growth, and we do not have to consider intercellular signaling since nuclei are not yet surrounded by membranes during the syncytial blastoderm stage (Campos-Ortega and Hartenstein, 1985). Lastly, patterning systems along the anteroposterior (A–P) and the dorsoventral (D–V) axes are largely independent of each other in the segmented germ band region of the blastoderm. Therefore, blastoderm nuclei, which are the basic objects of the gene circuit model, are arranged in a one-dimensional row along the A–P axis.

Gap gene circuits cover cleavage cycles 13 and 14A during the late syncytial blastoderm stage (Figure 2B; Foe and Alberts, 1983), including most of embryonic stages four and five in Campos-Ortega and Hartenstein (1985). This covers the time between the first unambiguous detection of zygotically expressed Kr and Gt proteins in early cycle 13 (our own data and Gaul and Jäckle, 1987; Eldon and Pirrotta, 1991; Kraut and Levine, 1991b), and the onset of gastrulation at the end of cycle 14A (Foe and Alberts, 1983). All nuclei divide equally and simultaneously at the beginning of cycle 14A.

Change in concentrations of transcription factors within each nucleus is governed by regulated protein synthesis, protein decay and diffusion between neighboring nuclei (Mjolsness

et al., 1991; REINITZ and SHARP, 1995). Due to the lack of an *in vitro* polymerase II assay for eukaryotic transcription which faithfully reproduces *in vivo* transcriptional regulation, it is currently impossible to formulate a gene network model based on mechanistic chemical kinetics of transcription. Instead, we use coarse-grained kinetic equations for protein concentrations which approximate the exact biochemistry with a sigmoid regulation-expression function (Figure 2C; MJOLSNESS *et al.*, 1991; REINITZ and SHARP, 1995).

Note that the general modeling framework outlined above does not specify which specific regulatory interactions take place within a gap gene circuit. These interactions are determined by regulatory parameters which constitute a genetic interconnectivity matrix (the T matrix). Each regulatory effect of a specific transcription factor on a target gene is described by a single parameter in the T matrix (Figure 2D). The gene circuit method aims to determine regulatory parameters and thus regulatory interactions within a gene circuit from given gene expression data. In other words, we seek sets of regulatory parameters that cause the gene circuit model to produce expression patterns that resemble real gap gene expression patterns as closely as possible (Figure 2A). This is achieved by fitting the model to quantitative segmentation gene expression data.

The set of quantitative gene expression data used in this study contains data for *bcd*, *cad*, *hb*, *Kr*, *kni*, *gt* and *tll* from wild type embryos (Figure 1; POUSTELNIKOVA *et al.*, 2004). Data and model can be compared by numerically calculating expression patterns for given time classes from the model, and then evaluating the sum of squared differences between model output and expression data for each gene, nucleus and time class for which we have data. We minimize this sum by using a global optimization method called Parallel Lam Simulated Annealing (PLSA, Figure 2A; CHU *et al.*, 1999). The optimization procedure results in a gene circuit, which is defined by a specific set of regulatory parameters. Due to the stochastic nature of PLSA, different gene circuits (*i.e.* different sets of parameters) may be obtained, which all show essentially correct gene expression patterns.

The last step of the gene circuit method is the analysis of gene circuits to gain biological insights. The most important aspect of the gene circuit method considered here is that it allows for very detailed analysis of direct regulatory interactions within a given gene network. This is achieved by studying the distribution of gene circuit parameters between different gene circuits, and by graphical analysis of regulatory contributions to specific patterning features (see RESULTS and REINITZ and SHARP, 1995). This method of analysis allows us to study quantitative regulatory contributions to gene regulation in any nucleus at any point in time during a simulation.

Here we present a dynamical analysis of the gap gene network based on gap gene circuits. We show that these circuits are able to reproduce gap gene expression patterns in the late Drosophila blastoderm at high accuracy and temporal resolution. We provide a detailed analysis of regulatory interactions involved in gap gene regulation and show that our results are largely consistent with existing experimental evidence. Our models extend current knowledge of the gap gene system in several important aspects. We predict an activating effect of Cad on *Kr*, and clarify evidence on the effects of Hb on *Kr*, Kr on *kni*, and Gt on *kni*. Our results suggest that mutual repression by complementary gap genes is absolutely essential for correct gap gene expression. We observe spatial asymmetry with posterior dominance in repressive interactions among overlapping gap genes. Moreover, the gene circuit method can provide information on regulatory mechanisms which is difficult to obtain by current experimental methods. Control of the posterior boundaries of posterior *kni* and *gt* was found to involve a temporal succession of multiple repressive interactions. Lastly, we report a correlation between regulatory input from the terminal maternal system and late formation of gap gene domain boundaries in the posterior region of the embryo.

MATERIALS AND METHODS

The gene circuit modeling framework: The gene circuit modeling framework has been described in detail in Mjolsness *et al.* (1991) and Reinitz and Sharp (1995). The basic objects of the gene circuit model are blastoderm nuclei denoted by the index i. We consider a one-dimensional model in which nuclei are arranged in a row along the A–P axis where nuclei $i-1$ and $i+1$ are neighbors of nucleus i. The model has three rules governing the behavior of nuclei in time t: (1) interphase, (2) mitosis and (3) division. Rules (1) and (2) are continuous and describe the dynamics of protein synthesis and decay within a nucleus, and protein diffusion between nuclei. Rule (3) is discrete and describes how each nucleus is replaced by its two daughter nuclei upon division. The schedule for these rules is based on Foe and Alberts (1983) and is summarized in Figure 2B.

The internal state of nucleus i is described by concentrations v_i^a of transcription factors encoded by segmentation genes denoted by index a. The change in transcription factor concentration over time dv_i^a/dt depends on three processes during interphase: (1) protein synthesis, (2) protein diffusion and (3) protein decay, represented by the summation terms on the right hand side of equation (1) below. During mitosis, protein synthesis is shut down and only diffusion and decay occur. Thus we write

$$\frac{dv_i^a}{dt} = R_a g\left(\sum_{b=1}^{N} T^{ab} v_i^b + m^a v_i^{\mathrm{Bcd}} + h^a\right) + D^a(n)\left[(v_{i-1}^a - v_i^a) + (v_{i+1}^a - v_i^a)\right] - \lambda_a v_i^a, \qquad (1)$$

where N is the total number of zygotic genes in the model.

In equation (1), T^{ab} represents a matrix of regulatory coefficients where each coefficient T^{ab} characterizes the regulatory effect of the product of gene b on the expression of gene a (Figure 2D). This matrix is independent of i reflecting the fact that each nucleus contains a copy of the same genome. v_i^{Bcd} is the concentration of Bcd in nucleus i. Bcd is exclusively maternal and its concentration is constant in time. The regulatory effect of Bcd on gene a is represented by the parameter m^a. h^a is a threshold parameter representing

regulatory contributions of uniformly expressed maternal transcription factors. The relative rate of protein synthesis is then given by the sigmoid regulation-expression function $g(u^a) = \frac{1}{2}\left[\left(u^a/\sqrt{(u^a)^2+1}\right)+1\right]$, where $u^a = \sum_{b=1}^{N} T^{ab} v_i^b + m^a v_i^{\mathrm{Bcd}} + h^a$ is the total regulatory input on gene a (Figure 2C). The maximum synthesis rate for the product of gene a is given by R^a. The diffusion parameter $D^a(n)$ depends on the number of nuclear divisions n that have taken place before the current time t. Diffusion is assumed to vary inversely with the square of the distance between neighboring nuclei and this distance is halved upon nuclear division. λ_a is the decay rate of the product of gene a. It is related to the protein half life of the product of gene a by $t^a_{1/2} = \ln 2/\lambda_a$.

Quantitative expression data: *Drosophila melanogaster* blastoderm stage embryos were fluorescently stained for Eve protein and two other gene products using antibodies described in KOSMAN *et al.* (1998). As secondary antibodies, we used FITC anti-guinea pig, Texas Red anti-rabbit, and Cy5 anti-rat. Laterally oriented embryos were scanned using the 16x oil immersion objective of a Leica TCS4D confocal laser microscope. Fluorescent dyes were excited with a single wavelength at a time to ensure no leakage between channels, using the BP-FITC filter for the 488 nm excitation line (FITC), the BP-60030 filter with for 568 nm (Texas Red), and the RG665 filter for 647 nm (Cy5). Expression levels were normalized per gene to a relative fluorescence intensity range of 0-255 based on the most intensely fluorescent pattern on each slide with multiple embryos. Embryo images were cropped to fit embryo size and aligned along the A–P axis as shown in Figure 1.

Image segmentation: A detailed description of this processing step can be found at `http://flyex.ams.sunysb.edu/flyex/proc_steps/dave.html`. Embryo images were segmented to obtain tabulated protein concentrations per nucleus as follows: Binary nuclear masks were constructed by edge detection, and average protein concentrations were obtained by averaging pixel values covering each nucleus in the mask. Nuclear positions are based on centroids of nuclei in the binary mask.

Time classification: Embryos were assigned to cleavage cycle 12 (time class: C12, used for initial conditions of the model at $t = 0.0$), cycle 13 (C13), and eight time classes (T1–T8) in cycle 14A (Figure 2B). Time classification for C12 and C13 is based on embryo morphology, and for T1–T8 on careful visual inspection of the highly dynamic *eve* expression pattern by two independent observers (D. KOSMAN, S. SURKOVA; *cf.* MYASNIKOVA *et al.*, 2001). Time classification was validated by membrane morphology (*cf.* MERRILL *et al.*, 1988), as well as automated classification of *eve* expression patterns by complex-valued neural networks (AIZENBERG *et al.*, 2002), and support-vector regression (MYASNIKOVA *et al.*, 2002).

Background removal/registration: Non-specific background staining was approximated by a paraboloid and subsequently eliminated by a linear mapping of intensities which transforms fluorescence at or below background level to zero and transforms maximum fluorescence to itself (MYASNIKOVA *et al.*, 2004). Expression patterns were registered using fast dyadic wavelets to align expression patterns as closely as possible (MYASNIKOVA *et al.*, 2001). Only nuclei with positional values in the middle 10% along the D–V axis were used for further processing.

Integrated data: Each integrated expression profile is based on registered data from at least ten embryos stained for a specific gene at a specific time class, with the exception of Kni at C13, which is based on only two embryos, and Tll, for which we did not have data earlier than T3. Nuclei were categorized into 25 (C12), 50 (C13) and 100 (T1–T8) equal-sized bins according to their position along the A–P axis (*cf.* FOE and ALBERTS, 1983). Concentration values for all nuclei in each bin were averaged to yield the final integrated one-dimensional expression pattern (Figure 1; POUSTELNIKOVA *et al.*, 2004). The concentration of Bcd v_i^{Bcd} is nearly constant with respect to time during cycles 13 and 14A, and is based on averaged registered *bcd* expression data from T1–T7. Concentrations of Cad and Hb at the onset of cycle 13 are derived from expression data for cycle 12. Initial concentrations for Kr, Kni, Gt and Tll are zero in all nuclei.

Optimization by Parallel Lam Simulated Annealing: PLSA was used as described in REINITZ and SHARP (1995) and CHU *et al.* (1999). The set of ordinary differential equations (1) was solved numerically using a Bulirsch-Stoer adaptive-step-size solver scheme adapted from PRESS *et al.* (1992). Equations were solved to a relative accuracy of 0.1%, and solutions were tested for numerical stability. We minimize the following cost function by adjusting parameters R_a, T^{ab}, m^a, h^a, D^a and λ_a in equation (1):

$$E = \sum \left(v_i^a(t)_{\text{model}} - v_i^a(t)_{\text{data}}\right)^2 .$$

Summation is performed over the total number of data points N_d, *i.e.* the number of protein measurements across all genes a, nuclei i and time classes t.

Parameter search spaces were defined by explicit search limits for R_a, D^a and λ_a and a collective penalty function for T^{ab}, m^a, h^a as described in REINITZ and SHARP (1995). h^a parameters of *Kr*, *kni*, *gt* and *hb* were fixed to negative values representing a constitutive 'off' state of the gene. This accelerated the annealing process considerably and slightly improved annealing results while not altering the overall quality of the resulting gene circuits. Optimization was performed in parallel on 10 2.4Ghz Pentium P4 Xeon processors and took between 8 and 160 hours per optimization run.

Selection of gap gene circuits: We use the root mean square (rms) score

$$\text{rms} = \sqrt{\frac{E}{N_d}}$$

as a measure for the quality of a gene circuit. The rms represents the average absolute difference between protein concentrations in model and data. PLSA is a stochastic optimization method yielding gap gene circuits of varying quality. Gene circuits most faithfully reproducing gap gene expression were selected as follows: First, only circuits with an rms of less than 12.0 were considered (20 circuits out of 40). All gap gene circuits with an rms of more than 12.0 showed obvious pattern defects, some of them severe such as displaced or missing expression boundaries. Second, each of the selected 20 circuits was carefully tested for

patterning defects by visual inspection and plotting of squared differences between model and data for each protein and time class. The 10 resulting circuits are listed in Table 1. Unless noted otherwise, graphs shown below use circuit 28008 (Table 2), since it has no circuit-specific patterning defects and its regulatory parameters correspond to the gap gene network topology observed in a majority of circuits (compare Table 2A to Figure 4A).

Analysis of circuit parameters: Parameters values T^{ab} and m^a were classified into three types of regulatory interaction: (1) repression for parameter values $\leq$ –0.005, (2) no interaction for parameter values between –0.005 and 0.005, or (3) activation for parameters ≥ 0.005 (see Figure 4A). The threshold of 0.005 for the 'no interaction' category was chosen empirically. Interactions falling into the 'no interaction' category usually had no detectable effect on pattern formation in gap gene circuits analyzed graphically (see below). The gap gene network topology observed in a majority of gap gene circuits (Figure 4A) is preserved if a threshold of 0.01 is used instead (data not shown).

Software and bioinformatics: Simulator and optimization code were implemented in C, data quantification tools were implemented in C and the Khoros image analysis environment, gene circuit analysis and plotting tools were implemented in Perl and Java. Software and gene circuit files are available at `http://flyex.ams.sunysb.edu/lab/gaps.html`. Expression data (FlyEx database) is available at `http://urchin.spbcas.ru/flyex`, and `http://flyex.ams.sunysb.edu/flyex`.

RESULTS

Ten gap gene circuits including *bcd*, *cad*, *hb*, *Kr*, *gt*, *kni* and *tll*, and covering a range of 35%–92% A–P position, were selected for analysis as described in MATERIALS AND METHODS (Table 1). A comparison between model output and quantified expression data is shown in Figure 3. Most circuits show minor circuit-specific patterning defects consisting of small spurious domains or slight irregularities in specific domain boundaries (Table 1). Moreover, all gap gene circuits show slight defects in the establishment of the posterior borders of the posterior *gt* and *hb* domains, and fail to reproduce the late parasegment 4 (PS4) specific expression peak of *hb* (Figure 3). Lastly, we observed slightly elevated expression levels of gap genes during early cycle 13 (data not shown).

Analysis of circuit parameters: The distribution of parameter values between circuits can vary from parameter to parameter (Figure 4). Most parameters show a strong tendency toward a particular type of regulatory interaction, *i.e.* activation, repression or no interaction. Figure 4A shows the gap gene network topology corresponding to genetic interactions observed in a majority of gap gene circuits (see Figure 9, for a schematic representation of the network). Although a gene circuit using average parameter values does not produce correct gap gene expression patterns (data not shown), we have found two circuits (26003, 28008) whose parameters exactly represent the topology of the majority of circuits (Table 2).

Some basic features of the gap gene network topology are immediately obvious from inspection of Figure 4A. First, Bcd and Cad generally activate zygotic gap gene expression. Second, *hb*, *Kr*, *kni* and *gt* show autoactivation. Third, except for autoregulatory interactions and the effect of Gt on *hb*, all reciprocal interactions among gap genes are either zero or repressive. Especially strong constraints for mutual repression are present between *Kr* and *gt*, as well as *kni* and *hb*, which show complementary expression patterns in the region of 35%–92% A–P position (Figure 1G–L). Many repressive interactions between overlapping

gap genes show weaker constraints toward repression, and we have found very weak or no dynamical constraints for repression of *kni*, *gt* and *hb* by the products of their immediate anterior neighbors *Kr*, *kni* and *gt* respectively. Lastly, the terminal gap gene product Tll represses all other gap genes except *hb*.

Graphical analysis of gap gene regulation: Graphical analysis of gap gene circuits allows us to 'dissect' regulatory contributions of different transcription factors on the expression of a target gene, and to characterize these interactions at great detail in space and time. To achieve this, we plot individual contributions to the sum of regulatory interactions affecting a gene's expression. Thereby, we focus on regions of expression domain boundaries. We identify regulatory factors responsible for the positioning of specific boundaries by looking for regulatory inputs that change significantly and consistently over the region of an expression domain boundary (*cf.* Reinitz and Sharp, 1995). Consistent change implies that for boundary control by activation, the activator has to show a spatial expression gradient of the same polarity as the boundary it controls. Analogously, boundary control by repression implies a gradient of repressor with opposite polarity to the boundary it controls.

We have found activation of gap genes by Bcd and Cad in broad regions of the embryo (Figure 5). Bcd contributes strong activating inputs on the anterior domains of *gt* (Figure 5A,C) and *hb* (Figure 5E,F,H,I) as well as the central domain of *Kr* (Figure 5B,D). Smaller activating inputs by Bcd can be detected in the posterior domains of *kni* (Figure 5G,J) and *gt* (Figure 5A,C). Three circuits (28003, 25005, 29007) show repression of *kni* by Bcd, suggesting that Bcd activation might not be essential for *kni* expression during cycle 14A (Figure 4A,C). The predominant maternal activating input on posterior *kni* and *gt* is provided by Cad (Figure 5C,J). Furthermore, Cad provides a relatively strong activating input to central *Kr* expression (Figure 5D), and even contributes significantly to early anterior expression of *hb* (Figure 5H). Note that a small activating contribution of Cad on anterior *hb* can be detected in most gap gene circuits, but the strong early activation of *hb*

by Cad shown in Figure 5H is exceptional. Activation in the posterior *hb* domain is largely due to Cad and *hb* autoactivation (Figure 4A,E and data not shown), a mechanism which we consider to be an artifact of the model (see DISCUSSION).

In addition to activation by maternal genes, zygotic gap genes show a tendency toward positive autoregulation (Figure 4). Autoactivation contributes strongly to zygotic expression of *Kr*, *hb* and *kni*, and can become the dominant activating contribution within an expression domain during the second half of cycle 14A (Figure 5D,I,J). Autoactivation of *gt* was found to be somewhat weaker (Figure 5C), and is not present at significant levels in all circuits (Figure 4A,D). Note that activation in the anterior *hb* domain is slightly special, due to the presence of maternally expressed Hb protein in the anterior half of the embryo (Figure 1B,E), which causes exceptionally strong autoactivation of *hb* early in cycle 14A (Figure 5H).

Whereas activation of gap genes by maternal genes occurs in rather broad regions, repressive interactions among gap genes provide spatially specific regulatory input for boundary positioning. Note that *Kr* and *gt* have mutually exclusive expression patterns in the blastoderm (Figure 1G–I, 6A). *Kr* shows repression by Gt in all circuits (Figure 4A,B). This repressive interaction is involved in positioning both anterior and posterior boundaries of central *Kr* expression during cycle 14A (Figure 6C). Although repression by Gt is quite strong, the regulatory profile of *Kr* indicates that missing repression by Gt does not lead to significant *Kr* derepression outside its central domain, since total regulatory input is not elevated significantly above the 10% level of expression in the absence of Gt (arrow in Figure 6C).

Both *hb* and *kni* show overlaps of their expression domains with the central domain of *Kr* (Figure 1I,L, 6B). Most circuits show repressive inputs on *Kr* by Hb and Kni which are weaker than that of Gt (Figure 4A,B). Kni is involved in setting the posterior border of the central *Kr* domain. Figure 6D (asterisk) shows that Kr synthesis expands posteriorly in the absence of Kni. Similarly, Hb is involved in setting the anterior border of the central *Kr*

domain, as Kr synthesis expands anteriorly in the absence of Hb (asterisk in Figure 6D). We found one circuit (28005) in which the boundaries of the *Kr* domain are set exclusively by Gt. However, this caused a slight patterning defect of the posterior *Kr* boundary at late cycle 14A (Table 1). In addition to the repressive interactions described above, we observe strong repression of *Kr* by Tll in all circuits (Figure 4A,B). This repression is not involved in setting the boundaries of the central *Kr* domain since it only affects regulation of *Kr* at the posterior pole of the embryo (data not shown).

The anterior border of the posterior *kni* domain (Figure 1L, 7A,B) is set by a combination of repressive inputs by Hb and Kr (Figure 7C,D). Whereas Hb represses *kni* in all circuits, repression by Kr was only observed in six out of ten circuits (Figure 4A,C). Gap gene circuits without repression of *kni* by Kr show no detectable defects in *kni* expression (data not shown). Regulation of the posterior border of *kni* reveals a dynamic succession of repressive interactions during cycle 14A (Figure 7E,F). All circuits show diminishing repressive input on *kni* by Tll in the region of the posterior boundary during cycle 14A (Figure 7E,F), as *tll* expression is only retained in a region posterior of 80% A–P position (compare Figure 7A and B). In contrast, there is increasing repression by Gt and Hb in the boundary region (Figure 7E,F). Note that the strength of repressive inputs by Gt and Tll varies greatly between circuits (Figure 4C, 7E,F). For instance, circuit 28008 (Figure 7E) shows extraordinarily strong repression of Gt, while other circuits such as 26001 show predominant repression by Hb and Tll, with a smaller contribution by Gt (Figure 7F).

gt is expressed in two domains in the region covered by gap gene circuits (Figure 1I, 8A). The posterior boundary of the anterior domain as well as the anterior boundary of the posterior domain of *gt* depend almost exclusively on very strong repression by Kr (Figure 8C). We detect a small repressive contribution by Hb to the anterior *gt* domain. However, Hb repression is not specifically involved in positioning the posterior boundary of this domain, being uniformly distributed across it (Figure 8E,F). In all circuits, the posterior border of

posterior *gt* is initially established through repression by Tll (Figure 8E). During cycle 14A, repression by Tll is increasingly complemented and replaced by Hb repression (Figure 8F). We found one circuit (28002) which shows weak activation of *gt* by Hb. This is likely to be an artifact of this particular circuit, since its posterior domain of *tll* was expanded slightly anteriorly to compensate for missing repression by Hb. Only one circuit (25005) showed very weak repression of *gt* by Kni, whereas all other circuits showed no such interaction (Figure 4A,D).

hb has an anterior and a posterior expression domain (Figure 1L, 8B). Regulation of *hb* is quite different from other gap genes in that it only has one repressive input (Figure 4A,E). Very strong repression of *hb* by Kni was found in all 10 circuits (Figure 4E). This repression is involved in positioning of the posterior border of the anterior *hb* domain as well as the anterior border of the posterior *hb* domain (Figure 8D). Note that we have found no effect of Kr on *hb* in any gap gene circuit (Figure 4A).

DISCUSSION

Accuracy and specificity of gap gene circuits: Some earlier models of gap gene expression did not consider the genetic nature of the underlying dynamic mechanism (Nagorcka, 1988; Goodwin and Kauffman, 1990; Hunding *et al.*, 1990). Others were based on generalized genetic mechanisms, which did not consider the specific dynamics of gene regulation or details of gap gene network topology (Meinhardt, 1986, 1988). As more detailed evidence became available, theoretical approaches incorporated more detailed, qualitative representations of gap gene regulation (Burstein, 1995; Sanchez and Thieffry, 2001; Tchuraev and Galimzyanov, 2001). The gene circuit method is the only approach so far, which allows for detailed quantitative analysis of dynamic regulatory interactions among gap genes. However, earlier studies using gap gene circuits showed a high degree of variation in the distribution of regulatory parameters between circuits (Reinitz *et al.*, 1995; Reinitz and Sharp, 1995). The quantitative data set used in the current study (Poustelnikova *et al.*, 2004) has resulted in several significant improvements. Error in gap gene expression patterns has been reduced to less than 5% deviation from gene expression data (Table 1), which is comparable with the experimental error in the data itself (Myasnikova *et al.*, 2001). The dynamics of gap gene expression are now reproduced to a temporal resolution of under seven minutes during cycle 14A. Our models show correct timing of gap gene expression and correct extents of overlaps between neighboring gap domains, two features of gap gene expression which were not addressed in earlier studies. Moreover, gap gene circuits reproduce shifts of gap domain boundaries during cycle 14A, a phenomenon first discovered by analyzing quantitative gap gene expression data (Jaeger *et al.*, 2004). Lastly, the addition of *cad* and *tll* has allowed us to extend the region for which we obtain correct gap gene expression patterns toward the posterior pole region.

Some theoretical approaches to regulatory interactions in the segmentation gene network

infer these interactions based on interpretation of mutant expression patterns taken from the literature (Sanchez and Thieffry, 2001; Kumar *et al.*, 2002). A difficulty with this approach is that such models tend to reproduce the interpretations of data they are based on, rather than providing an independent interpretation. In contrast, the gene circuit method does not require any *a priori* assumptions about specific regulatory interactions. Instead, it attempts to reconstruct these interactions based on wild type gene expression data (Figure 2A). Given this caveat, it is noteworthy that the results of our analysis of the gap gene network are largely consistent with studies based on mutant gene expression (see below). The fact that two independent methods lead to very similar results is an important cross-validation of conclusions based on both approaches.

Fitting models with many parameters to data is always at risk of producing non-specific results. Gap gene circuits fail to fit expression data in regions of the embryo where additional factors are required for regulation, *i.e.* anterior of about 35% A–P position (*cf.* Reinitz *et al.*, 1995), where gap gene regulation is known to involve head gap genes (Cohen and Jürgens, 1990; Finkelstein and Perrimon, 1990; Grossniklaus *et al.*, 1994), and posterior of 92% A–P position, where activity of the terminal gap gene *hkb* is required (Weigel *et al.*, 1990; Brönner and Jäckle, 1991). Moreover, even though we have not obtained unique values for regulatory parameters in different circuits, we have found a strong tendency toward a specific type of regulatory interaction for most parameters (Figure 4). This suggests that gap gene circuits represent the gap gene regulatory network in a specific and reproducible way.

Mechanisms of Gap Gene Regulation: Although activating contributions from Bcd and Cad show some degree of localization (Figure 5), positioning of gap gene boundaries during cycle 14A is largely under the control of repressive gap-gap cross-regulatory interactions. Thereby, activation is a prerequisite for repressive boundary control, which counteracts broad activation of gap genes in a spatially specific manner (Figures 5–8). In addition, gap genes

show a tendency toward autoactivation (Figure 4), which increasingly potentiates activation by Bcd and Cad during cycle 14A (Figure 5). Autoactivation is involved in maintenance of gap gene expression within given domains and sharpening of gap domain boundaries during cycle 14A. A similar, but less specific mechanism for spatially localized gene activation by maternal gradients has been proposed by MEINHARDT (1988).

Regulatory loops of mutual repression create positive regulatory feedback between complementary gap genes providing a straightforward mechanism for their mutually exclusive expression patterns. Such a mechanism of 'alternating cushions' of gap domains has been proposed by KRAUT and LEVINE (1991a) and CLYDE *et al.* (2003). Our results suggest that this mechanism is complemented by repression among overlapping gap genes. Overlap in expression patterns of two repressors imposes a limit on the strength of repressive interactions between them. Accordingly, repression between neighboring gap genes is generally weaker than between complementary ones (Figure 4). Moreover, repression among overlapping gap genes is asymmetric, centered on the *Kr* domain (see Figure 9). Posterior of this domain, only posterior neighbors contribute functional repressive inputs to gap gene expression, while anterior neighbors do not. We show elsewhere that this asymmetry is responsible for anterior shifts of posterior gap gene domains during cycle 14A (JAEGER *et al.*, 2004).

Repression by Tll mediates regulatory input to gap gene expression by the terminal maternal system (see INTRODUCTION). Tll provides the main repressive input to early regulation of the posterior boundary of posterior *gt* (Figure 8E), and activation by Tll is required for posterior *hb* expression (REINITZ and LEVINE, 1990; CASANOVA, 1990; BRÖNNER and JÄCKLE, 1991). Note that these two features only form during cycle 13 and early cycle 14A (Figure 3), while other gap domain boundaries are already present at the transcript level during cycles 10–12 (KNIPPLE *et al.*, 1985; TAUTZ, 1988; ROTHE *et al.*, 1989; MOHLER *et al.*, 1989) and largely depend on the anterior and posterior maternal systems for their initial establishment (TAUTZ, 1988; MOHLER *et al.*, 1989; GAUL and JÄCKLE,

1987; Rivera-Pomar *et al.*, 1995). The delayed formation of posterior patterning features and their distinct mode of regulation are reminiscent of segment determination in primitive dipterans and intermediate germ band insects, supporting a conserved dynamical mechanism across different insect taxa (Tautz and Sommer, 1995; Davis and Patel, 2002).

The set of regulatory interactions presented here provides a consistent and sufficient dynamical mechanism for gap gene expression (see Introduction). In summary, this set of interactions consists of the following five basic regulatory mechanisms (Figure 9): (1) Broad activation by Bcd and/or Cad, (2) autoactivation, (3) strong repressive feedback between mutually exclusive gap genes, (4) asymmetric repression between overlapping gap genes and (5) feed-forward repression of posterior domain boundaries by the terminal gap gene *tll*. In the following subsections, we discuss evidence concerning specific regulatory interactions involved in each of these basic mechanisms in some detail.

Activation by Bcd and Cad: Activation of gap gene expression by Bcd and Cad is supported by the following. Bcd binds to the regulatory regions of *hb*, *Kr* and *kni* (Driever and Nüsslein-Volhard, 1989; Driever *et al.*, 1989; Hoch *et al.*, 1991; Rivera-Pomar *et al.*, 1995). The *kni* regulatory region also contains binding sites for Cad (Rivera-Pomar *et al.*, 1995). The anterior domains of *gt* and *hb* are absent in embryos from *bcd* mothers (Tautz, 1988; Eldon and Pirrotta, 1991). The posterior domain of *gt* is missing in embryos mutant for both maternal and zygotic *cad*, while the posterior domain of *kni* is absent in embryos mutant for maternal *bcd* plus maternal and zygotic *cad* (Rivera-Pomar *et al.*, 1995). Our results suggest partial redundancy of activation of *kni* by Bcd, consistent with evidence from zygotic *cad* embryos from *bcd* mothers, where maternally provided Cad is sufficient to activate *kni* (Rivera-Pomar *et al.*, 1995).

Kr expression expands anteriorly in embryos from *bcd* mothers (Gaul and Jäckle, 1987), which is due to the absence of the anterior *gt* and *hb* domains (Tautz, 1988; Eldon and Pirrotta, 1991; Kraut and Levine, 1991a). Bcd has been shown to activate ex-

pression of *Kr* reporter constructs (HOCH *et al.*, 1990, 1991) supporting an activating effect of Bcd on endogenous *Kr*. The fact that *Kr* is still expressed in embryos from *bcd* mutant mothers has been attributed to activation by general transcription factors (KERRIGAN *et al.*, 1991) or low levels of Hb (HÜLSKAMP *et al.*, 1990; STRUHL *et al.*, 1992; SCHULZ and TAUTZ, 1994). In contrast, our models predict that this activation is provided by Cad (Figure 4A,B, 5D). Although *Kr* expression is normal in embryos overexpressing *cad* (MLODZIK *et al.*, 1990), repressive control of *Kr* boundaries could account for the lacking expansion of the *Kr* domain in such embryos.

The activating effect of Cad on *hb* found in gap gene circuits is likely to be spurious. The anterior *hb* domain is absent in embryos from *bcd* mutant mothers (TAUTZ, 1988) which show uniformly high levels of Cad (MLODZIK and GEHRING, 1987). Moreover, the complete absence of the posterior *hb* domain in *tll* mutants (REINITZ and LEVINE, 1990; CASANOVA, 1990; BRÖNNER and JÄCKLE, 1991) suggests activation of posterior *hb* by Tll rather than Cad. We believe that this spurious activation of *hb* by Cad is due to the absence of *hkb* in gap gene circuits. The posterior *hb* domain fails to retract from the posterior pole in *hkb* mutants (CASANOVA, 1990; BRÖNNER and JÄCKLE, 1991) suggesting a repressive role of Hkb in regulation of the posterior *hb* border. Consistent with this, the posterior boundary of the posterior *hb* domain never fully forms in any of our circuits (Figure 3). Moreover, Tll is constrained to a very small or no interaction with *hb* (Figure 4E) due to the absence of the posterior repressor Hkb, since activation of *hb* by Tll would lead to increasing *hb* expression extending to the posterior pole.

Autoactivation: A role for autoactivation in the late phase of *hb* regulation (SCHRÖDER *et al.*, 1988; HÜLSKAMP *et al.*, 1994) is supported by the fact that the posterior border of anterior *hb* is shifted anteriorly in a concentration-dependent manner in embryos with decreasing doses of zygotic Hb (SIMPSON-BROSE *et al.*, 1994). Weakened and narrowed expression of *Kr* in mutants encoding a functionally defective Kr protein (WARRIOR and

Levine, 1990) suggests *Kr* autoactivation. Similarly, a delay in the expression of *gt* in mutants encoding a defective Gt protein (Eldon and Pirrotta, 1991) indicates *gt* autoactivation. However, our results suggest that *gt* autoactivation is not essential. It is generally weaker than autoactivation of other gap genes (Figure 4B–E), and circuits lacking *gt* autoactivation show no specific defects in *gt* expression. Lastly, in the case of *kni*, there is no experimental evidence for autoactivation, while some authors have even suggested *kni* autorepression (Howard, 1990; Rothe *et al.*, 1994). We have not been able to detect such autorepression in any gap gene circuit (Figure 4A,C).

Repression between complementary gap genes: Mutual repression of *gt* and *Kr* is supported by the following. *gt* expression expands into the region of the central *Kr* domain in *Kr* embryos (Eldon and Pirrotta, 1991; Kraut and Levine, 1991b). In contrast, *Kr* expression is not altered in *gt* mutants before germ band extension (Gaul and Jäckle, 1987; Reinitz and Levine, 1990; Eldon and Pirrotta, 1991). However, Gt binds to the *Kr* regulatory region (Capovilla *et al.*, 1992), and the central domain of *Kr* is absent in embryos overexpressing *gt* (Kraut and Levine, 1991a). Moreover, *Kr* expression extends further anterior in *hb gt* double mutants than in *hb* mutants alone (Kraut and Levine, 1991a). The above is consistent with our analysis, which shows no significant derepression of *Kr* in the absence of Gt even though repression of *Kr* by Gt is quite strong (Figure 6C).

Hb binds to the *kni* regulatory region, and the posterior *kni* domain expands anteriorly in *hb* mutants (Hülskamp *et al.*, 1990; Rothe *et al.*, 1994; Clyde *et al.*, 2003). Embryos overexpressing *hb* show no *kni* expression at all (Nauber *et al.*, 1988; Rothe *et al.*, 1989; Kraut and Levine, 1991a), and embryos misexpressing *hb* show spatially specific repression of *kni* expression (Clyde *et al.*, 2003). There is no clear posterior expansion of *kni* in *hb* mutants (Hülskamp *et al.*, 1990; Clyde *et al.*, 2003). This could be due to the relatively weak and late repressive contribution of Hb on the posterior *kni* boundary, or due to partial redundancy with repression by Gt and Tll (Figure 7E,F). The posterior *hb* domain expands

anteriorly in *kni* mutants, but anterior *hb* expression is not altered in these embryos (JÄCKLE *et al.*, 1986; CLYDE *et al.*, 2003). Nevertheless, a role of Kni in positioning the anterior *hb* domain is suggested by the fact that misexpression of *kni* leads to spatially specific repression of both anterior and posterior *hb* domains (KOSMAN and SMALL, 1997; WU *et al.*, 2001; CLYDE *et al.*, 2003). Moreover, only slight posterior expansion of anterior *hb* is observed in *Kr* mutants, while *hb* is completely derepressed between its anterior and posterior domains in *Kr kni* double mutants (CLYDE *et al.*, 2003).

Repression between overlapping gap genes: gt, *kni* and *Kr* show repression by their immediate posterior neighbors *hb*, *gt* and *kni* respectively (Figure 4). Retraction of posterior Gt from the posterior pole during mid cycle 14A fails to occur in *hb* mutants (MOHLER *et al.*, 1989; ELDON and PIRROTTA, 1991; KRAUT and LEVINE, 1991b), and no *gt* expression is observed in embryos overexpressing *hb* (ELDON and PIRROTTA, 1991; KRAUT and LEVINE, 1991a). The posterior *kni* boundary is shifted posteriorly in *gt* mutant embryos (ELDON and PIRROTTA, 1991), and *kni* expression is reduced in embryos overexpressing *gt* (CAPOVILLA *et al.*, 1992). Note that these effects are very subtle and were not reported in similar studies by different authors (KRAUT and LEVINE, 1991a; ROTHE *et al.*, 1994). A weak but functional interaction of Gt with *kni* is consistent with our results. This interaction was found to be essential even in a circuit (29007) where it was deemed below significance level (Figure 4A,C and data not shown). Lastly, Kni has been shown to bind to the *Kr* regulatory region (HOCH *et al.*, 1992), and the central *Kr* domain expands posteriorly in *kni* mutants (JÄCKLE *et al.*, 1986; GAUL and JÄCKLE, 1987).

In contrast, we have been unable to detect any effect of Kr on *hb* (Figure 4A,B). However, *hb* expression expands posteriorly in *Kr* mutants (JÄCKLE *et al.*, 1986; GAUL and JÄCKLE, 1989; CLYDE *et al.*, 2003). This effect is likely to involve repression of *hb* by Kni. Kni levels are reduced in *Kr* embryos (PANKRATZ *et al.*, 1989). *hb* is completely derepressed between its anterior and posterior domains in *Kr kni* double mutants, whereas anterior *hb* does not

expand at all in *kni* mutants alone (CLYDE *et al.*, 2003). Taken together with our results, this suggests that there is direct repression of *hb* by Kr in the embryo, but it is at least partially redundant with repression of *hb* by Kni.

Unlike repression by posterior neighbors, we have found no or only weak repression of posterior *kni*, *gt* and *hb* by their anterior neighbors *Kr*, *kni* and *gt* respectively (Figure 4). Most gap gene circuits show weak activation of *hb* by Gt (Figure 4A,E). Graphical analysis failed to reveal any functional role for such activation (Figure 5H,I). Moreover, we have found no functional interaction between *gt* and Kni (Figure 4A,D). Although relatively weak repression of *kni* by Kr was found in six out of ten circuits (Figure 4A,C), no specific patterning defects could be detected in the other four. Consistent with the above, expression of posterior *hb* is normal in *gt* mutants, and both the anterior boundaries of posterior *gt* and *kni* are positioned correctly in *kni* and *Kr* mutant embryos respectively (MOHLER *et al.*, 1989; PANKRATZ *et al.*, 1989; ELDON and PIRROTTA, 1991; ROTHE *et al.*, 1994).

Note that we have never observed activation of *kni* by Kr (Figure 4A,C), which has been proposed to explain decreased expression levels of *kni* in *Kr* mutants (PANKRATZ *et al.*, 1989; ROTHE *et al.*, 1994). Our results strongly support the view that this interaction is indirect through Gt, which is further corroborated by the fact that *kni* expression is completely restored in *Kr gt* double mutants compared to *Kr* mutants alone (CAPOVILLA *et al.*, 1992).

We have found a significant repressive effect of Hb on *Kr* (Figure 4A,B). Consistent with this, Hb has been shown to bind to the *Kr* regulatory region (HOCH *et al.*, 1991), and the central *Kr* domain expands anteriorly in *hb* mutants (JÄCKLE *et al.*, 1986; GAUL and JÄCKLE, 1987). However, partial redundancy of this interaction is suggested by correct positioning and shape of the anterior *Kr* domain in a circuit (28005) which does not show repression of *Kr* by Hb (Table 1).

It has been proposed that Hb plays a dual role as both activator and repressor of *Kr* (see INTRODUCTION). In the framework of the gene circuit model, concentration-dependent

switching of regulative action could be implemented by allowing genetic interconnection parameters to switch sign at certain regulator concentration thresholds. Our current model explicitly does not include such a possibility. Nevertheless, we have been able to obtain circuits that reproduce *Kr* expression faithfully (Figure 3) suggesting that a dual role of Hb is not required for proper *Kr* expression. Moreover, we have never observed activation of *Kr* by Hb in any of the circuits (Figure 4A,B). Therefore, our results support a mechanism in which the activation of *Kr* by Hb is indirect through derepression of *kni*.

Repression by Tll: Only few earlier theoretical approaches have considered terminal gap genes (Meinhardt, 1986; Tchuraev and Galimzyanov, 2001). Gap gene circuits accurately reproduce *tll* expression (data not shown). However, in gene circuits, *tll* is subject to regulation by other gap genes which is inconsistent with experimental evidence (Brönner and Jäckle, 1991). In contrast, the correct expression pattern of *tll* in gap gene circuits allows us to study its effect on other gap genes in great detail. We have found strong repressive effects of Tll on *Kr*, *kni* and *gt* (Figure 4). Tll binding sites have been found in the regulatory regions of *Kr* (Hoch *et al.*, 1992) and *kni* (Pankratz *et al.*, 1992). In *tll* mutants, *Kr* expression is normal (Gaul and Jäckle, 1987; Reinitz and Levine, 1990), whereas expression of *kni* expands posteriorly (Pankratz *et al.*, 1989), and the posterior *gt* domain fails to retract from the posterior pole (Eldon and Pirrotta, 1991; Kraut and Levine, 1991b). No expression of *Kr*, *kni* or *gt* can be detected in embryos overexpressing *tll* under a heat shock promoter (Steingrimsson *et al.*, 1991; Kraut and Levine, 1991a).

Comparison to logical analysis: The logical analysis by Sanchez and Thieffry (2001) is the only other theoretical study of the gap gene system which achieves a level of detail comparable to the analysis presented here. Our results largely agree with Sanchez and Thieffry (2001), with the following notable exceptions. *tll* and the posterior *hb* domain were not considered in the logical analysis. The absence of posterior *hb* could explain why Sanchez and Thieffry (2001) did not report a repressive feedback loop between *hb* and

kni, which we have found to be essential for gap gene regulation. Moreover, a difficulty with logical analysis is that functional thresholds must be assigned to continuous protein concentrations prior to the analysis. This leads to assigning functional borders of expression domains in the embryo which may not coincide with observable expression borders. In the case of SANCHEZ and THIEFFRY (2001), *a priori* assignment of thresholds implicitly results in the posterior borders of the anterior *hb* domain, central *Kr* domain, and central *kni* domain coinciding, while the posterior domains of *kni* and *gt* show no overlap (*cf.* Figure 1I,L). The authors conclude that a dual role of Hb in *Kr* regulation is required to account for the large overlap between the two respective expression domains. Our expression data indicate that the posterior *hb* boundary (Figure 1I,L) lies in the middle of the *Kr* domain, and our analysis suggests that a dual role of Hb is not required for correct expression of *Kr*. Lastly, the discrete logical approach failed to reveal the role of autoactivation in sharpening gap domain boundaries during cycle 14A. The thresholds selected by SANCHEZ and THIEFFRY (2001) divided the embryo into four discrete zones along the A–P axis, but modeling boundary sharpening requires an approach with a larger spatial resolution.

Limitations of the model: We observe artificially high levels of gap proteins during early cycle 13 (data not shown) and earlier cleavage cycles if included in the model (REINITZ *et al.*, 1995, and data not shown). This is a serious problem for analysis of early gap gene regulation, since premature accumulation of gap proteins causes premature gap-gap regulatory interactions which rapidly dominate early inputs from maternal genes. In the embryo, production delays between the time when a transcription factor binds to a regulatory region and the completion of subsequent protein synthesis, have a significant influence on the timing of gene expression (ROTHE *et al.*, 1992). Cleavage cycles 10–12 are only about 7–13 minutes long, which is significantly shorter than cycles 13 and 14A (FOE and ALBERTS, 1983). A production delay on a scale of 5-15 minutes combined with transcript degradation during mitosis (SHERMOEN and O'FARRELL, 1991) can account for the absence of zygotic

gap proteins before cycle 13. Therefore, production delays will have to be incorporated into gap gene circuits to obtain correct early gap gene expression and regulation.

Gene circuits can be used for prediction of expression patterns in mutants (Sharp and Reinitz, 1998). Mild changes in genotype, such as varying Bcd dosage, led to successful prediction of mutant gap gene expression patterns using gap gene circuits (Simpson-Brose *et al.*, 1994; Reinitz *et al.*, 1995). In contrast, we have not been able to predict gap gene expression patterns in null mutants. This could be due to spurious early gap gene regulation (see above). Alternatively, it might be due to scaling indeterminacy in our quantitative expression data. We currently do not know the proportionality constant, different for each protein, that relates fluorescence levels with absolute protein concentrations. Just as improvements in the data used in the present study improved results over previous studies, we expect that further improvements in data quantification will lead to further improvement in the predictive capacity of our models.

Our analysis yields a much more dynamic picture of gap gene expression than previously thought. During the late blastoderm stage, gap gene expression patterns and their regulatory interactions change on a very rapid scale. Many open questions remain about how or if the transient and highly dynamic nature of these patterns and interactions affects the establishment of the stable segmentation prepattern of segment polarity gene expression. To address these questions, future gene circuit models will have to include more downstream layers of the segmentation gene network, namely pair-rule and segment-polarity genes. Just as the gap gene system is only the first step in the regulatory hierarchy of the segmentation gene system, our current models are only the first step toward more comprehensive gene circuit models of segment determination in *Drosophila melanogaster*.

We would like to thank Hilde Janssens, Nick Monk, Julia Dallman and James Baker for discussions and comments on the manuscript. This work was supported by the National Institutes of Health, Grants RR07801 and TW01147, and by CRDF GAP Award RBO-1286.

LITERATURE CITED

Aizenberg, I., E. Myasnikova, M. Samsonova, and J. Reinitz, 2002 Temporal classification of *drosopila* segmentation gene expression patterns by the multi-valued neural recognition method. Mathematical Biosciences **176**: 145–159.

Akam, M., 1987 The molecular basis for metameric pattern in the *drosophila* embryo. Development **101**: 1–22.

Brönner, G. and H. Jäckle, 1991 Control and function of terminal gap gene activity in the posterior pole region of the *drosophila* embryo. Mechanisms of Development **35**: 205–211.

Burstein, Z., 1995 A network model of developmental gene hierarchy. The Journal of Theoretical Biology **174**: 1–11.

Campos-Ortega, J. A. and V. Hartenstein, 1985 *The Embryonic Development of* Drosophila melanogaster. Springer, Heidelberg, Germany.

Capovilla, M., E. D. Eldon, and V. Pirrotta, 1992 The *giant* gene of *drosophila* encodes a b-ZIP DNA-binding protein that regulates the expression of other segmentation gap genes. Development **114**: 99–112.

Casanova, J., 1990 Pattern formation under the control of the terminal system in the *drosophila* embryo. Development **110**: 621–628.

Chu, K. W., Y. Deng, and J. Reinitz, 1999 Parallel simulated annealing by mixing of states. The Journal of Computational Physics **148**: 646–662.

Clyde, D. E., M. S. G. Corado, X. Wu, A. Paré, D. Papatsenko, and S. S., 2003 A self-organizing system of repressor gradients establishes segmental complexity in *drosophila*. Nature **426**: 849–853.

Cohen, S. M. and G. Jürgens, 1990 Mediation of *drosophila* head development by gap-like segmentation genes. Nature **346**: 482–485.

Davis, G. K. and N. H. Patel, 2002 Short, long and beyond: Molecular and embryological approaches to insect segmentation. Annual Reviews in Entomology **47**: 669–699.

Driever, W. and C. Nüsslein-Volhard, 1989 The Bicoid protein is a positive regulator of *hunchback* transcription in the early *drosophila* embryo. Nature **337**: 138–143.

Driever, W., G. Thoma, and C. Nüsslein-Volhard, 1989 Determination of spatial domains of zygotic gene expression in the *drosophila* embryo by the affinity of binding sites for the Bicoid morphogen. Nature **340**: 363–367.

Eldon, E. D. and V. Pirrotta, 1991 Interactions of the *drosophila* gap gene *giant* with maternal and zygotic pattern-forming genes. Development **111**: 367–378.

Finkelstein, R. and N. Perrimon, 1990 The *orthodenticle* gene is regulated by *bicoid* and *torso* and specifies *drosophila* head development. Nature **346**: 485–488.

Foe, V. E. and B. M. Alberts, 1983 Studies of nuclear and cytoplasmic behaviour during the five mitotic cycles that precede gastrulation in *drosophila* embryogenesis. The Journal of Cell Science **61**: 31–70.

Frasch, M. and M. Levine, 1987 Complementary patterns of *even-skipped* and *fushi-tarazu* expression involve their differential regulation by a common set of segmentation genes in *drosophila*. Genes and Development **1**: 981–995.

Gaul, U. and H. Jäckle, 1987 Pole region-dependent repression of the *drosophila* gap gene *krüppel* by maternal gene products. Cell **51**: 549–555.

Gaul, U. and H. Jäckle, 1989 Analysis of maternal effect mutant combinations elucidates regulation and function of the overlap of *hunchback* and *krüppel* gene expression in the *drosophila* blastoderm embryo. Development **107**: 651–662.

Goodwin, B. C. and S. A. Kauffman, 1990 Spatial harmonics and pattern specification in early *drosophila* development. I: Bifurcation sequences and gene expression. The Journal of Theoretical Biology **144**: 303–319.

Grossniklaus, U., K. M. Cadigan, and W. J. Gehring, 1994 Three maternal coordinate systems cooperate in the patterning of the *drosophila* head. Development **120**: 3155–3171.

Harding, K. and M. Levine, 1988 Gap genes define the limits of antennapedia and bithorax gene expression during early development in *drosophila*. The EMBO Journal **7**: 205–214.

Hoch, M., N. Gerwin, H. Taubert, and H. Jäckle, 1992 Competition for overlapping sites in the regulatory region of the *drosophila* gene *krüppel*. Science **256**: 94–97.

Hoch, M., C. Schröder, E. Seifert, and H. Jäckle, 1990 Cis-acting control elements for *krüppel* expression in the *drosophila* embryo. The EMBO Journal **9**: 2587–2595.

Hoch, M., E. Seifert, and H. Jäckle, 1991 Gene expression mediated by cis-acting sequences of the *krüppel* gene in response to the *drosophila* morphogens Bicoid and Hunchback. The EMBO Journal **10**: 2267–2278.

Howard, K., 1990 The blastoderm prepattern. Seminars in Cell Biology **1**: 161–172.

Hülskamp, M., W. Lukowitz, A. Beermann, G. Glaser, and D. Tautz, 1994 Differential regulation of target genes by different alleles of the segmentation gene *hunchback* in *drosophila*. Genetics **138**: 125–134.

Hülskamp, M., C. Pfeifle, and D. Tautz, 1990 A morphogenetic gradient of Hunchback protein organizes the expression of the gap genes *krüppel* and *knirps* in the early *drosophila* embryo. Nature **346**: 577–580.

Hunding, A., S. A. Kauffman, and B. C. Goodwin, 1990 *Drosophila* segmentation: Supercomputer simulation of prepattern hierarchy. The Journal of Theoretical Biology **145**: 369–384.

Ingham, P. W., 1988 The molecular genetics of embryonic pattern formation in *drosophila*. Nature **335**: 25–34.

Jäckle, H., D. Tautz, R. Schuh, E. Seifert, and R. Lehmann, 1986 Cross-regulatory interactions among the gap genes of *drosophila*. Nature **324**: 668–670.

Jaeger, J., S. Surkova, M. Blagov, D. Kosman, K. N. Kozlov, Manu, E. Myasnikova, C. E. Vanario-Alonso, M. Samsonova, D. H. Sharp, and J. Reinitz, 2004 Dynamic control of positional information in the early *drosophila* embryo. Nature **submitted**.

Kerrigan, L. A., G. E. Croston, L. M. Lira, and J. T. Kadonaga, 1991 Sequence-specific transcriptional antirepression of the *drosophila krüppel* gene by the GAGA factor. The Journal of Biological Chemistry **266**: 574–582.

Knipple, D. C., E. Seifert, U. B. Rosenberg, A. Preiss, and H. Jäckle, 1985 Spatial and temporal patterns of *krüppel* gene expression in early *drosophila* embryos. Nature **317**: 40–44.

Kosman, D. and S. Small, 1997 Concentration-dependent patterning by an ectopic expression domain of the *drosophila* gap gene *knirps*. Development **124**: 1343–1354.

Kosman, D., S. Small, and J. Reinitz, 1998 Rapid preparation of a panel of polyclonal antibodies to *drosophila* segmentation proteins. Development, Genes and Evolution **208**: 290–294.

Kraut, R. and M. Levine, 1991a Mutually repressive interactions between the gap genes *giant* and *krüppel* define middle body regions of the *drosophila* embryo. Development **111**: 611–621.

Kraut, R. and M. Levine, 1991b Spatial regulation of the gap gene *giant* during *drosophila* development. Development **111**: 601–609.

Kumar, S., K. Jayaraman, S. Panchanathan, R. Gurunathan, A. Marti-Subirana, and S. J. Newfeld, 2002 BEST: A novel computational approach for comparing gene expression patterns from early stages of *drosophila melanogaster* development. Genetics **162**: 2037–2047.

Meinhardt, H., 1986 Hierarchical inductions of cell states: A model for segmentation in *drosophila*. The Journal of Cell Science (Supplement) **4**: 357–381.

Meinhardt, H., 1988 Models for maternally supplied positional information and the activation of segmentation genes in *drosophila* embryogenesis. Development (Supplement) **104**: 95–110.

Merrill, P. T., D. Sweeton, and E. Wieschaus, 1988 Requirements for autosomal gene activity during precellular stages of *drosophila melanogaster*. Development **104**: 495–509.

Mjolsness, E., D. H. Sharp, and J. Reinitz, 1991 A connectionist model of development. The Journal of Theoretical Biology **152**: 429–453.

Mlodzik, M. and W. J. Gehring, 1987 Hierarchy of the genetic interactions that specify the anteroposterior segmentation pattern of the *drosophila* embryo as monitored by *caudal* protein expression. Development **101**: 421–435.

Mlodzik, M., G. Gibson, and W. J. Gehring, 1990 Effects of ectopic expression of *caudal* during *drosophila* development. Development **109**: 271–277.

Mohler, J., E. D. Eldon, and V. Pirrotta, 1989 A novel spatial transcription pattern associated with the segmentation gene, *giant*, of *drosophila*. The EMBO Journal **8**: 1539–1548.

Myasnikova, E., A. Samsonova, K. Kozlov, M. Samsonova, and J. Reinitz, 2001 Registration of the expression patterns of *drosophila* segmentation genes by two independent methods. Bioinformatics **17**: 3–12.

Myasnikova, E., A. Samsonova, M. Samsonova, and J. Reinitz, 2002 Support vector regression applied to the determination of the developmental age of a *drosophila* embryo from its segmentation gene expression patterns. Bioinformatics **18 (Suppl.)**: S87–S95.

Myasnikova, E., M. Samsonova, and J. Reinitz, 2004 Removal of background signal from *in situ* data on the expression of segmentation genes in *drosophila*. Bioinformatics **submitted**.

Nagorcka, B. N., 1988 A pattern formation mechanism to control spatial organization in the embryo of *drosophila melanogaster*. The Journal of Theoretical Biology **132**: 277–306.

Nauber, U., M. J. Pankratz, A. Kienlin, E. Seifert, U. Klemm, and H. Jäckle, 1988 Abdominal segmentation of the *drosophila* embryo requires a hormone receptor-like protein encoded by the gap gene *knirps*. Nature **336**: 489–492.

Nüsslein-Volhard, C., H. G. Frohnhofer, and R. Lehmann, 1987 Determination of anteroposterior polarity in *drosophila*. Science **238**: 1675–1687.

Nüsslein-Volhard, C. and E. Wieschaus, 1980 Mutations affecting segment number and polarity in *drosophila*. Nature **287**: 795–801.

Pankratz, M. J., M. Busch, M. Hoch, E. Seifert, and H. Jäckle, 1992 Spatial control of the gap gene *knirps* in the *drosophila* embryo by posterior morphogen system. Science **255**: 986–989.

Pankratz, M. J., M. Hoch, E. Seifert, and H. Jäckle, 1989 *Krüppel* requirement for *knirps* enhancement reflects overlapping gap gene activities in the *drosophila* embryo. Nature **341**: 337–340.

Poustelnikova, E., A. Pisarev, M. Blagov, M. Samsonova, and J. Reinitz, 2004 Flyex database. `http://urchin.spbcas.ru/flyex`.

Press, W. H., S. A. Teukolsky, W. T. Vetterling, and B. P. Flannery, 1992 *Numerical Recipes in C*. Cambridge University Press, Cambidge, U.K.

Reinitz, J., D. Kosman, C. E. Vanario-Alonso, and D. H. Sharp, 1998 Stripe forming architecture of the gap gene system. Developmental Genetics **23**: 11–27.

Reinitz, J. and M. Levine, 1990 Control of the initiation of homeotic gene expression by the gap genes *giant* and *tailless* in *drosophila*. Developmental Biology **140**: 57–72.

Reinitz, J., E. Mjolsness, and D. H. Sharp, 1995 Cooperative control of positional information in *drosophila* by *bicoid* and maternal *hunchback*. The Journal of Experimental Zoology **271**: 47–56.

Reinitz, J. and D. H. Sharp, 1995 Mechanism of *eve* stripe formation. Mechanisms of Development **49**: 133–158.

Rivera-Pomar, R., X. Lu, N. Perrimon, H. Taubert, and H. Jäckle, 1995 Activation of posterior gap gene expression in the *drosophila* blastoderm. Nature **376**: 253–256.

Rothe, M., U. Nauber, and H. Jäckle, 1989 Three hormone receptor-like *drosophila* genes encode an identical DNA-binding finger. The EMBO Journal **8**: 3087–3094.

Rothe, M., M. Pehl, H. Taubert, and H. Jäckle, 1992 Loss of gene function through rapid mitotic cycles in the *drosophila* embryo. Nature **359**: 156–159.

Rothe, M., E. A. Wimmer, M. J. Pankratz, M. González-Gaitán, and H. Jäckle, 1994 Identical transacting factor requirement for *knirps* and *knirps-related* gene expression in the anterior but not in the posterior region of the *drosophila* embryo. Mechanisms of Development **46**: 169–181.

Sanchez, L. and D. Thieffry, 2001 A logical analysis of the *drosophila* gap-gene system. The Journal of Theoretical Biology **211**: 115–141.

Schröder, C., D. Tautz, E. Seifert, and H. Jäckle, 1988 Differential regulation of the two transcripts from the *drosophila* gap segmentation gene *hunchback*. The EMBO Journal **7**: 2881–2887.

Schulz, C. and D. Tautz, 1994 Autonomous concentration-dependent activation and repression of *krüppel* by *hunchback* in the *drosophila* embryo. Development **120**: 3043–3049.

Sharp, D. H. and J. Reinitz, 1998 Prediction of mutant expression patterns using gene circuits. Biosystems **47**: 79–90.

Shermoen, A. W. and P. H. O'Farrell, 1991 Progression of the cell cycle through mitosis leads to abortion of nascent transcripts. Cell **97**: 303–310.

Simcox, A. A. and J. H. Sang, 1983 When does determination occur in *drosophila* embryos? Developmental Biology **97**: 212–221.

Simpson-Brose, M., J. Treisman, and C. Desplan, 1994 Synergy between the Hunchback and Bicoid morphogens is required for anterior patterning in *drosophila*. Cell **78**: 855–865.

Small, S., A. Blair, and M. Levine, 1996 Regulation of two pair-rule stripes by a single enhancer in the *drosophila* embryo. Developmental Biology **175**: 314–324.

St Johnston, D. and C. Nüsslein-Volhard, 1992 The origin of pattern and polarity in the *drosophila* embryo. Cell **68**: 201–219.

Steingrimsson, E., F. Pignoni, G. J. Liaw, and J. A. Lengyel, 1991 Dual role of the *drosophila* pattern gene *tailless* in embryonic termini. Science **254**: 418–421.

Struhl, G., P. Johnston, and P. A. Lawrence, 1992 Control of *drosophila* body pattern by the *hunchback* morphogen gradient. Cell **69**: 237–249.

Tautz, D., 1988 Regulation of the *drosophila* segmentation gene *hunchback* by two maternal morphogenetic centres. Nature **332**: 281–284.

Tautz, D. and R. J. Sommer, 1995 Evolution of segmentation genes in insects. Trends in Genetics **11**: 23–27.

Tchuraev, R. N. and A. V. Galimzyanov, 2001 Modeling of actual eukaryotic control gene subnetworks based on the method of generalized threshold models. Molecular Biology (Moscow) **35**: 1088–1094.

Warrior, R. and M. Levine, 1990 Dose-dependent regulation of pair-rule stripes by gap proteins and the initiation of segment polarity. Development **110**: 759–767.

Weigel, D., G. Jürgens, M. Klingler, and H. Jäckle, 1990 Two gap genes mediate maternal terminal pattern information in *drosophila*. Science **248**: 495–498.

Wu, X., V. Vasisht, D. Kosman, J. Reinitz, and S. Small, 2001 Thoracic patterning by the *drosophila* gap gene *hunchback*. Developmental Biology **237**: 79–92.

FIGURE LEGENDS

FIGURE 1.—Gene expression data before and after data processing. Confocal scans of immunofluorescently stained Drosophila blastoderm embryos (A–C,G,H,J,K), and quantified averaged expression graphs (D–F,I,L) are shown for Bcd (A,D), Hb (B,E) and Cad (C,F) at cleavage cycle 13 (time class: C13), and Gt (G,I), Kr (H,I), Hb (J,L) and Kni (K,L) at late cycle 14A (time class: T8). Anterior is to the left. Dorsal is up in embryo images. Graphs show relative protein concentration (with a range from 0 to 255 fluorescence units) plotted against relative position on the A–P axis (where 0% is the anterior pole). The gray shaded area indicates the region included in gap gene circuits (35%–92% A–P position). Embryo images taken from the FlyEx database. FlyEx embryo accession names: bd3 (A,C), hz30 (B), nk5 (G), kd17 (H), kf9 (J), fq1 (K). See MATERIALS AND METHODS for details.

FIGURE 2.—The gene circuit method. (A) The basic principle. Regulatory interactions are inferred from wild type expression patterns by fitting gene circuit models to quantitative data. (B) Time schedule for gap gene circuits. The model spans the time from the onset of cycle 13 (0.0 min) to the onset of gastrulation at the end of cycle 14A (71.1 min). The three rules of the model (interphase, mitosis and nuclear division) are shown to the right. There is one time class in cycle 13 (C13), and eight time classes (T1–T8) in cycle 14A. Time points used for comparison of model output to data for time classes C13 and T1–T8 are indicated. (C) The regulation-expression function $g(u)$. Total regulatory input u is shown on the horizontal axis. Corresponding relative activation of protein synthesis $g(u)$ is shown on the vertical axis. $g(u)$ rapidly approaches saturation for values of u above 1.5, and rapidly approaches zero for values of u below –1.5 (dashed lines). (D) Regulatory interactions within a gene circuit are represented by the genetic interconnection matrix T (shown here for interactions of *hb*, *Kr*, *gt* and *kni*). See text for details.

FIGURE 3.—Comparison between gene expression data and gene circuit model output. Expression patterns for the protein products of *Kr*, *kni*, *gt* and *hb* are shown at early (T1, upper), mid (T4, middle) and late cycle 14A (T8, lower row). Model output is represented by solid lines, gene expression data by dashed lines. The only obvious patterning defects affect the establishment of the posterior borders of *gt* and *hb* (asterisks) and the parasegment 4 (PS4) specific expression domain of *hb* at around 45% A–P position during late cycle 14A (arrow). Axes represent percent A–P position and relative protein concentration as described for Figure 1. See Figure 2B for time classes.

FIGURE 4.—Distribution of gene circuit parameters involved in the regulation of *hb*, *Kr*, *gt* and *kni* across all 10 gap gene circuits. (A) Classification of parameters by type of interaction. Number triplets show the number of gene circuits in which a parameter falls into each regulatory category (repression/no interaction/activation). Roman type indicates activation, gray type no interaction, and bold type repression in a majority of circuits. Table rows represent targets, columns represent regulators. (B–E) Scatter plots of m and T parameters for regulation of *Kr* (B), *kni* (C), *gt* (D) and *hb* (E). See Figure 2D and MATERIALS AND METHODS for parameter definition and principles of classification.

FIGURE 5.—Activation of *gt* (A,C), *Kr* (B,D), *hb* (E,F,H,I) and *kni* (G,J). (A,B,E,F,G) Modeled expression patterns of *cad*, *hb*, *Kr*, *kni* and *gt*, and expression data for *bcd* are shown at early (E, time class: T1) and late cycle 14A (A,B,F,G, T8). Axes as in Figure 3. (C,D,H,I,J) Activation profiles of *gt* (C), *Kr* (D), *hb* (H,I) and *kni* (J) at early (H, T1) and late cycle 14A (C,D,I,J, T8). Total regulatory input (u, solid black line) is plotted against percent A–P position. Colored areas represent individual regulatory contributions. The height of each colored area represents strength of activation as given by $m^a v_i^{\mathrm{Bcd}}$ for Bcd, and $T^{ab} v_i^b$, for any other factor b (see equation (1)). Dashed horizontal lines indicate regulatory

levels below which expression is at less than 10% (lower line), and above which expression is at more than 90% (upper line) of the maximal expression rate (see Figure 2C). Dashed vertical lines indicate A–P positions at which u^a falls below the 10% expression level.

FIGURE 6.—Repressive interactions involved in regulation of *Kr* domain boundaries. (A,B) Modeled expression patterns at late cycle 14A (T8). Axes as in Figure 3. (C,D) Repression profiles for *Kr* at late cycle 14A (T8). Total regulatory input u^{Kr} (solid black line) is plotted against percent A–P position. Colored areas represent individual regulatory contributions. Axes, dashed lines and definition of regulatory contributions as in Figure 5. Arrow in (C) indicates very slight level of derepression of *Kr* in the absence of Gt. Asterisks in (D) indicate shifts in the boundaries of the domain of Kr synthesis in the absence of Hb and Kni.

FIGURE 7.—Repressive interactions involved in regulation of *kni* domain boundaries. (A) Modeled expression patterns at early (A, T1) and late cycle 14A (B, T8). Axes as in Figure 3. (C,D) Spatial repression profiles for *kni* at early (T1, C) and late (T8, D) cycle 14A. (E,F) Temporal repression profiles of *kni* in a nucleus at 76% A–P position (dotted line in A–D) from circuit 28008 (E) and circuit 26001 (F). Mitosis is indicated by gray shaded background. (C–F) Total regulatory input u^{kni} is shown as a solid black line. Dashed lines and definition of regulatory contributions as in Figure 5.

FIGURE 8.—Repressive interactions involved in regulation of *gt* (A,C,E,F) and *hb* (B,D) domain boundaries. (A,B) Modeled expression patterns at late cycle 14A (T8). Axes as in Figure 3. (C) Strong repressive contribution of Kr on *gt* in the central region of the embryo at late cycle 14A (T8). (D) The only repressive input on *hb* found in gene circuits is strong repression by Kni, shown at late cycle 14A (T8). (E,F) Repressive regulatory contributions

of Hb and Tll on *gt* expression are shown at early (T1, E) and late (T8, F) cycle 14A. (C–F) Total regulatory input u is shown as a solid black line. Axes, definition of regulatory contributions and dashed lines as in Figure 5.

FIGURE 9.—Overview of the gap gene network. Expression domains of *hb*, *kni*, *gt*, *Kr*, and *Tll* are shown schematically as black boxes. Anterior is to the left. Regulatory interactions are based on Figure 4A. Only functional interactions present in at least 9 out of 10 gap gene circuits are shown. Repressive interactions are represented by T-bar connectors. Background shading represents main maternal activating inputs by Bcd (dark) and Cad (light). The gap gene network consists of five basic regulatory mechanisms: (1) Activation of gap genes by Bcd and/or Cad, (2) autoactivation, (3) strong repression between mutually exclusive gap genes, (4) repression between overlapping gap genes, (5) repression by Tll.

TABLES AND FIGURES

Table 1

Root mean square (rms) scores of gap gene circuits used in the analysis

Circuit	rms	Specific patterning defects
25003	10.335	anterior bulge in posterior *hb*
25005	11.143	very small spurious central *tll* domain
25010	10.880	very small spurious central *tll* domain
		early anterior bulge in posterior *gt*
26001	10.633	very small spurious central *tll* domain
26003	10.153	early anterior bulge in posterior *gt*
28002	10.288	slight anterior extension of *tll*
28005	10.108	posterior bulge in late *Kr*
		very small spurious central *tll* domain
28008	10.170	no specific defects detected
29002	10.137	very small spurious posterior *Kr* domain
		early anterior bulge in posterior *gt*
29007	9.420	no specific defects detected

Only circuit-specific pattern defects are listed here. Unless noted otherwise, circuit 28008 was used in all graphs shown below. See text for details.

Table 2A

Parameters of gap gene circuit 28008: Regulatory parameters

	Regulator gene b						
Target gene a	*bcd*	*cad*	*hb*	*Kr*	*gt*	*kni*	*tll*
cad	–0.040	–0.068	–0.073	–0.050	–0.056	–0.038	–0.034
hb	0.050	0.022	0.019	0.001	0.011	–0.166	0.003
Kr	0.129	0.033	–0.014	0.017	–0.076	–0.015	–0.080
gt	0.177	0.029	–0.018	–0.110	0.011	–0.001	–0.020
kni	0.097	0.037	–0.027	–0.024	–0.090	0.045	–0.077
tll	–0.007	–0.018	–0.106	–0.106	–0.082	–0.137	–0.003

Parameters displayed here correspond to m^a (for *bcd*) and T^{ab} (for all other regulator genes) in equation (1). Unless noted otherwise, this circuit was used in all graphs shown below.

Table 2B

Parameters of gap gene circuit 28008: Other parameters

	Gene a					
Parameter	*cad*	*hb*	*Kr*	*gt*	*kni*	*tll*
R_a	20.000	19.608	16.373	15.789	12.185	11.906
h^a $^{(*)}$	13.459	–3.500	–3.500	–3.500	–3.500	8.173
D^a	0.200	0.200	0.200	0.142	0.200	0.200
$t^a_{1/2}$	18.000	7.254	8.980	9.577	12.499	16.842

$^{(*)}$ h^a parameters for *hb*, *Kr*, *gt* and *kni* were fixed to –3.5 during optimization.

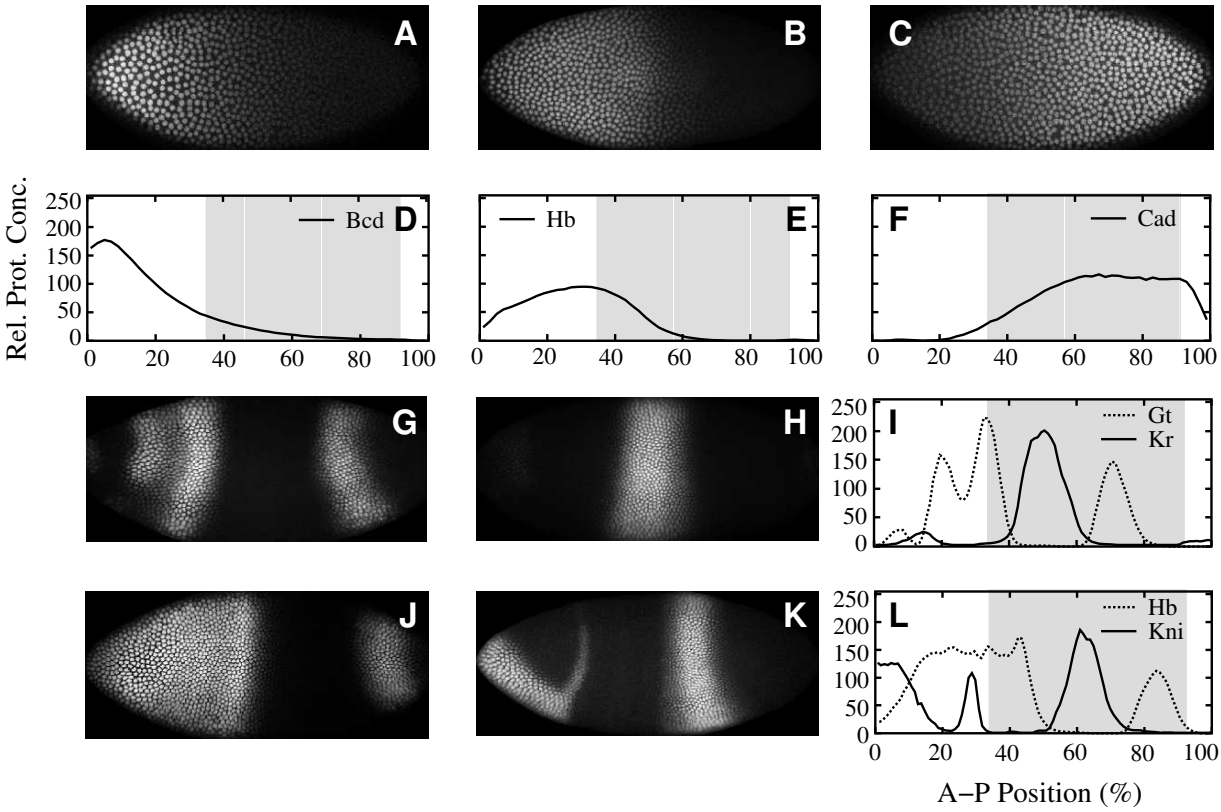
A
B
C
Rel. Prot. Conc.
250
200
150
100
50
0
Bcd
D
Hb
E
F
Cad
0
20
40
60
80
100
G
H
I
Gt
Kr
J
K
L
Hb
Kni
A–P Position (%)

FIGURE 1

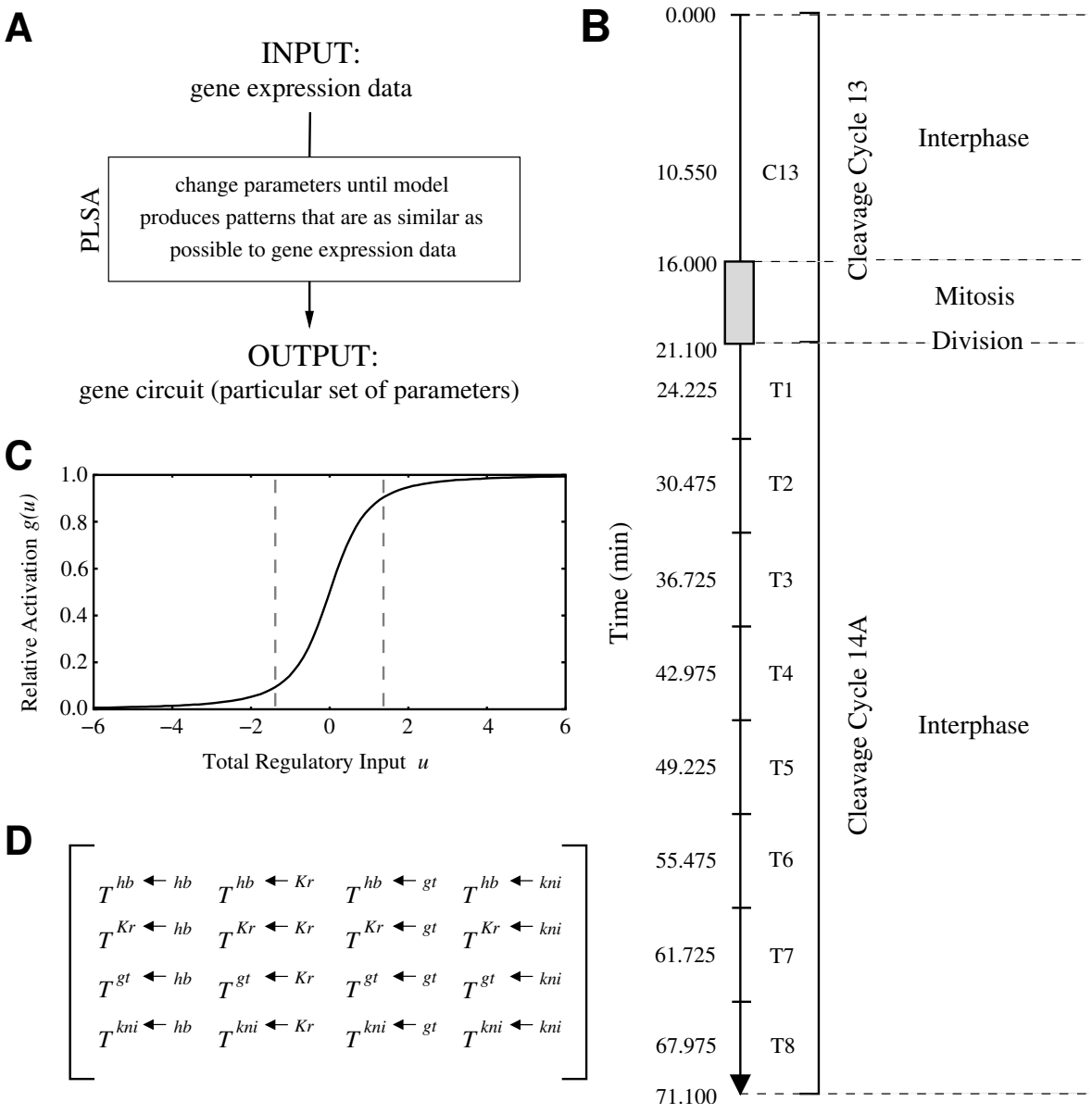
A
INPUT:
gene expression data
PLSA
change parameters until model
produces patterns that are as similar as
possible to gene expression data
OUTPUT:
gene circuit (particular set of parameters)
B
Time (min)
0.000
10.550
16.000
21.100
24.225
30.475
36.725
42.975
49.225
55.475
61.725
67.975
71.100
C13
T1
T2
T3
T4
T5
T6
T7
T8
Cleavage Cycle 13
Interphase
Mitosis
Division
Cleavage Cycle 14A
Interphase
C
Relative Activation g(u)
1.0
0.8
0.6
0.4
0.2
0.0
−6
−4
−2
0
2
4
6
Total Regulatory Input u
D
T hb ← hb
T hb ← Kr
T hb ← gt
T hb ← kni
T Kr ← hb
T Kr ← Kr
T Kr ← gt
T Kr ← kni
T gt ← hb
T gt ← Kr
T gt ← gt
T gt ← kni
T kni ← hb
T kni ← Kr
T kni ← gt
T kni ← kni

FIGURE 2

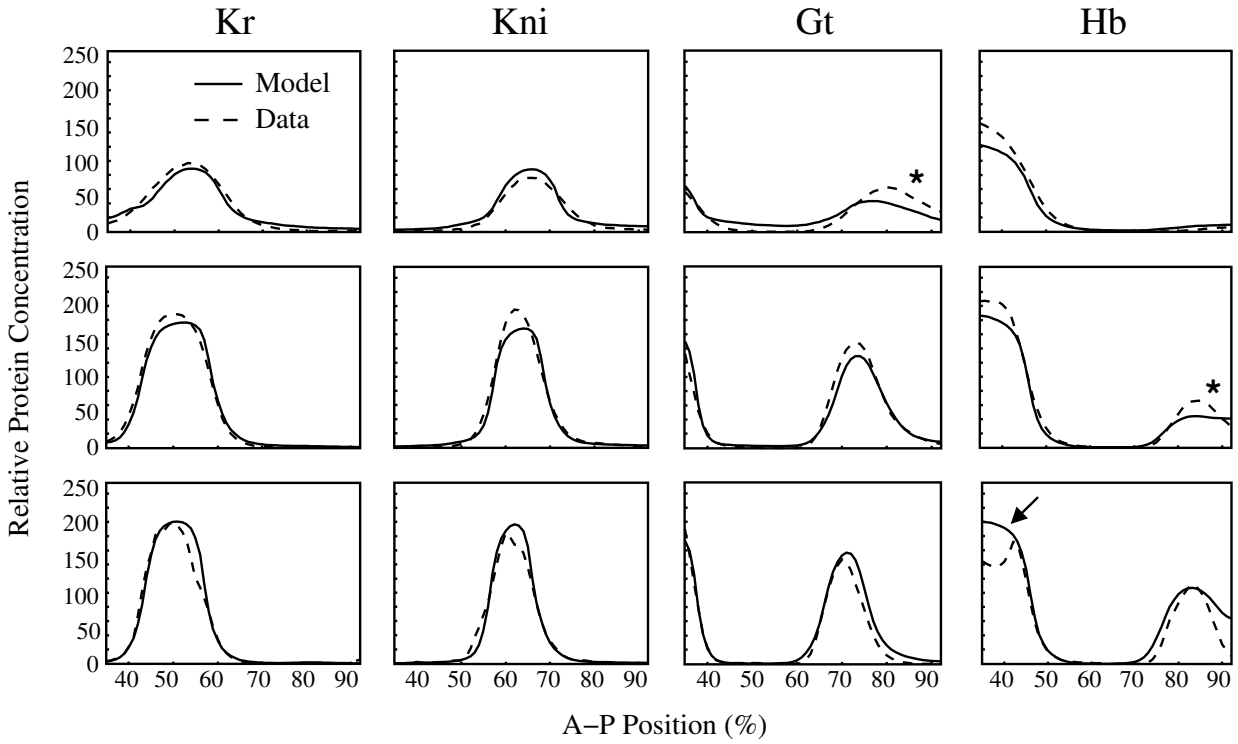
Kr
Kni
Gt
Hb
Model
Data
Relative Protein Concentration
A–P Position (%)
0
50
100
150
200
250
40
50
60
70
80
90

FIGURE 3

A

	bcd	*cad*	*hb*	*Kr*	*gt*	*kni*	*tll*
hb	0/0/10	0/0/10	0/0/10	0/10/0	0/2/8	**10/0/0**	1/8/1
Kr	0/0/10	0/0/10	**9/1/0**	0/0/10	**10/0/0**	**9/1/0**	**10/0/0**
gt	0/0/10	0/0/10	**9/0/1**	**10/0/0**	0/3/7	1/9/0	**10/0/0**
kni	3/0/7	0/0/10	**10/0/0**	**6/4/0**	**9/1/0**	0/0/10	**10/0/0**

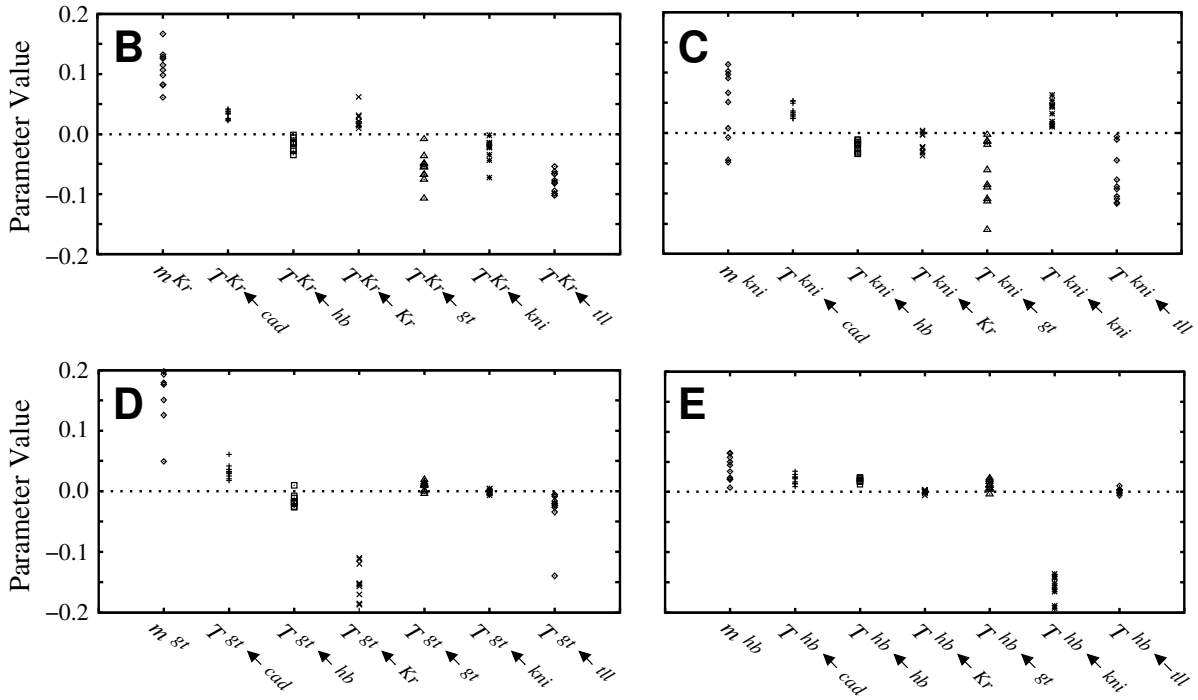

FIGURE 4

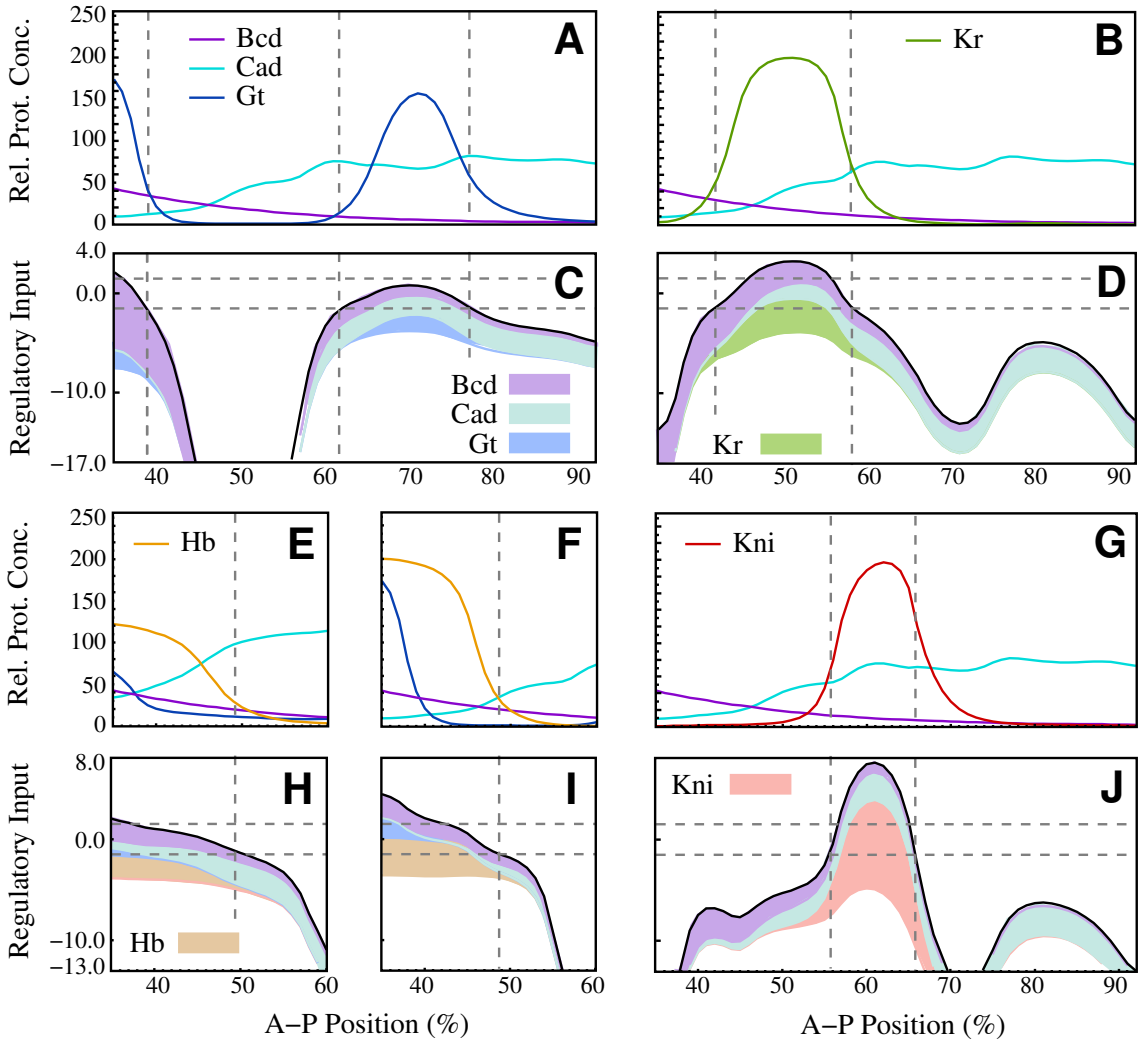
Rel. Prot. Conc.
Bcd
Cad
Gt
A
Kr
B
Regulatory Input
C
D
Hb
E
F
Kni
G
H
I
J
A–P Position (%)
A–P Position (%)

FIGURE 5

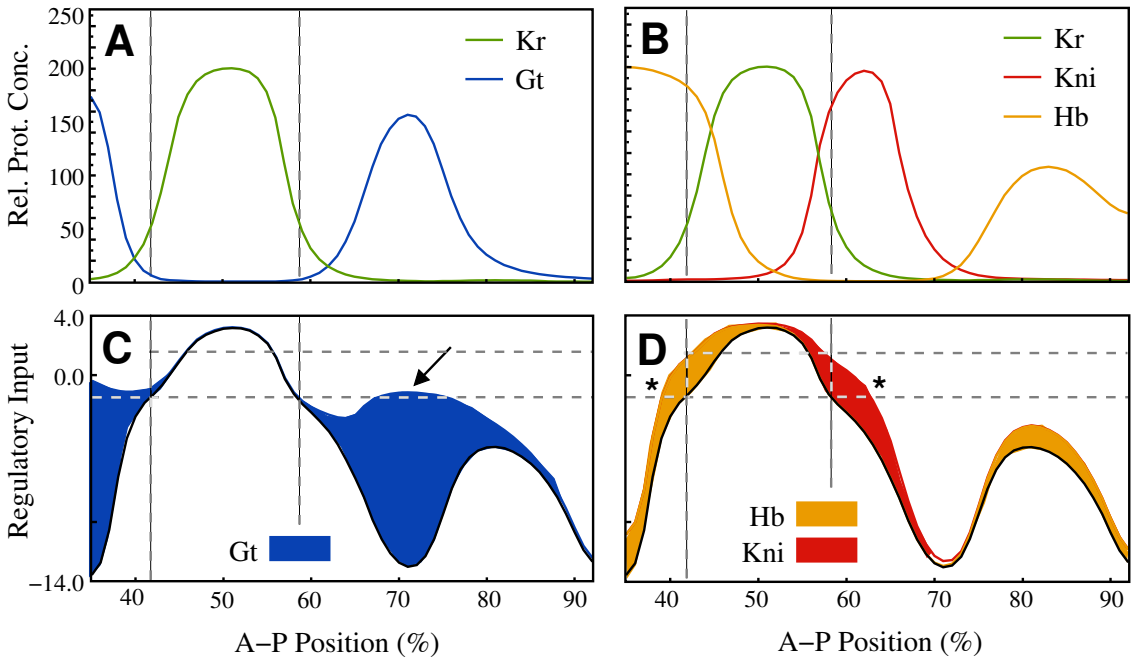
A
B
C
D
Kr
Gt
Kni
Hb
Rel. Prot. Conc.
250
200
150
100
50
0
Regulatory Input
4.0
0.0
−14.0
40
50
60
70
80
90
A–P Position (%)
*
*

FIGURE 6

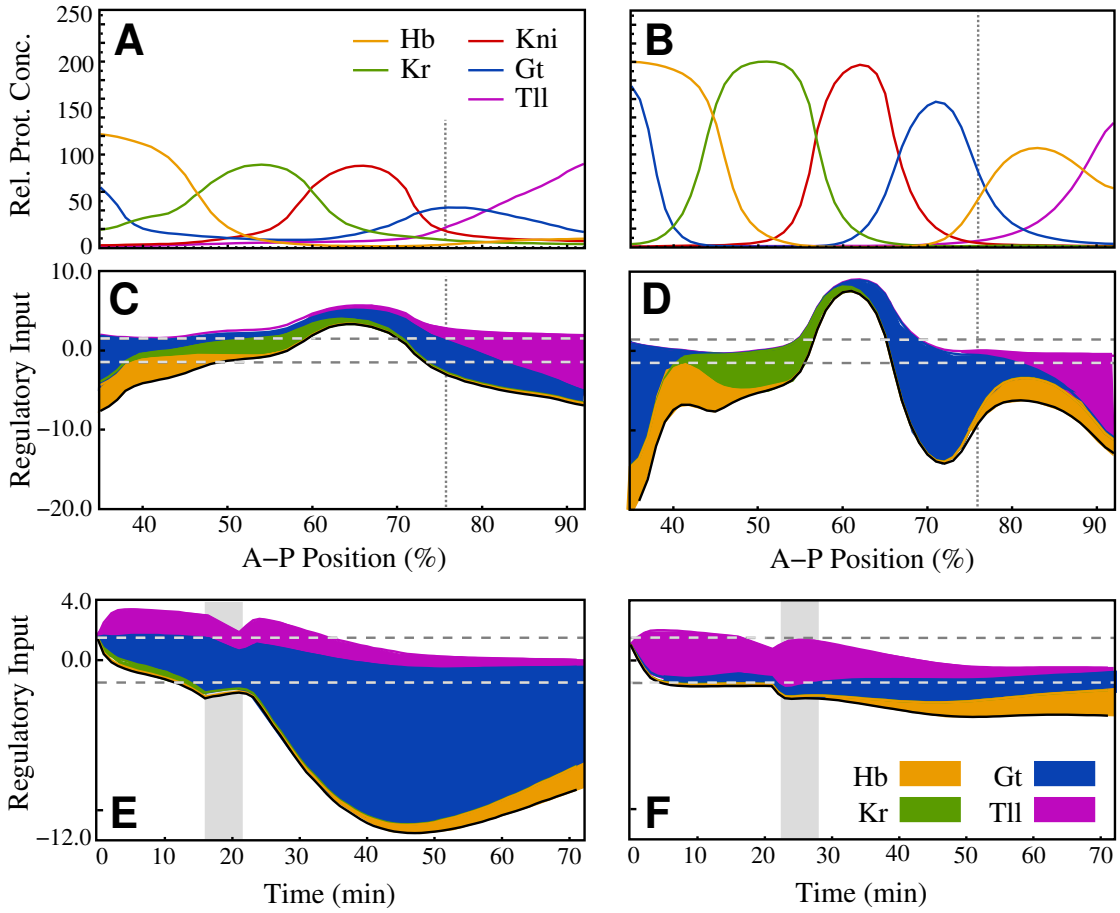
A
B
C
D
E
F
Hb
Kr
Kni
Gt
Tll
Rel. Prot. Conc.
Regulatory Input
A–P Position (%)
Time (min)

FIGURE 7

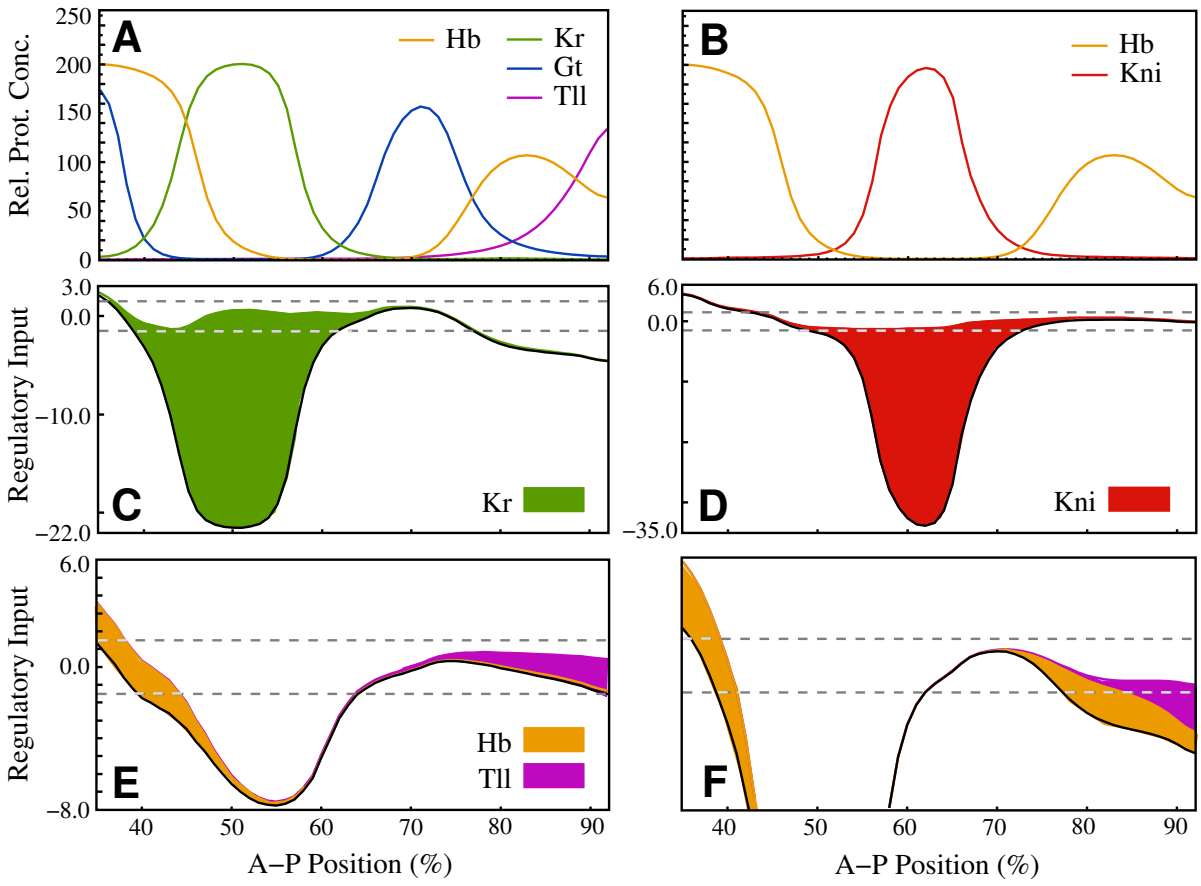
A
Hb
Kr
Gt
Tll
Rel. Prot. Conc.
250
200
150
100
50
0
B
Hb
Kni
C
Kr
Regulatory Input
3.0
0.0
−10.0
−22.0
D
Kni
6.0
0.0
−35.0
E
Hb
Tll
6.0
0.0
−8.0
F
40
50
60
70
80
90
A–P Position (%)

FIGURE 8

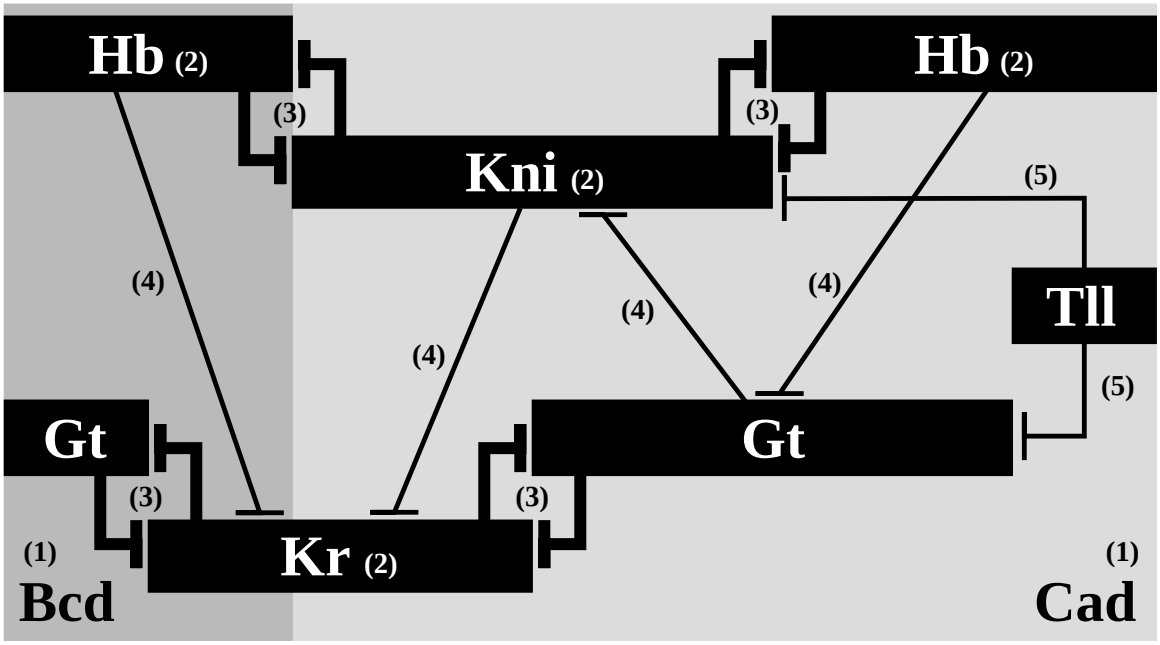

FIGURE 9